APPLICATION OF THEORETICAL DESIGN METHODS
TO THE STUDY OF PERFORMANCE LIMITS
OF AIRFOILS IN CASCADE

JOHN E. JENISTA

6

APPLICATION OF THEORETICAL DESIGN METHODS
TO THE STUDY OF PERFORMANCE LIMITS
OF AIRFOILS IN CASCADE

* * * * *

John E. Jenista

APPLICATION OF THEORETICAL DESIGN METHODS

TO THE STUDY OF PERFORMANCE LIMITS

OF AIRFOILS IN CASCADE

by

John E. Jenista

Lieutenant Commander, United States Navy

Submitted in partial fulfillment of
the requirements for the degree of

MASTER OF SCIENCE

IN

AERONAUTICAL ENGINEERING

United States Naval Postgraduate School
Monterey, California

1963

APPLICATION OF THEORETICAL DESIGN METHODS

TO THE STUDY OF PERFORMANCE LIMITS

OF AIRFOILS IN CASCADE

by

John E. Jenista

This work is accepted as fulfilling

the thesis requirements for the degree of

MASTER OF SCIENCE

IN

AERONAUTICAL ENGINEERING

from the

United States Naval Postgraduate School

ABSTRACT

A method of designing airfoils in cascade by means of conformal transformations is discussed. Design of these airfoils is regulated by five independent input parameters, with solutions obtained by digital computer. A large number of cascades generated by this method are compared. To evaluate the limits of performance, a parameter to indicate the tendency toward flow separation is introduced, with a limiting value established and verified. Proper solidity is shown to be of great importance in achieving low values of this separation parameter. The value of proper solidity for a given blade thickness is shown to be relatively independent of fairing shape. To increase performance, reducing blade thickness with a corresponding increase in solidity is shown to yield much greater improvement than changes in fairing shape.

TABLE OF CONTENTS

LIST OF ILLUSTRATIONS

TABLE OF SYMBOLS

Regular Symbol	Fortran Symbol	Explanation
x	XI(I)	Rectangular coordinates of ith point
y	YI(I)	in near circle plane
r	RI(I)	Polar coordinates of ith point in
λ	ALI(I)	near circle plane
v	VI(I)	Velocity and direction at i^{th} point
α	AHI(I)	in near circle plane
θ	TEI(I)	Angular coordinate if i^{th} point in circle plane
V_θ	VTI(I)	Velocity at i^{th} point in circle plane
ΔV_θ	DVI(I)	Velocity increment produced by circulation at i^{th} point in circle plane
ξ	XII(I)	Rectangular coordinates of ith point
η	ETI(I)	in cascade plane
α'	EPI(I)	Argument of conjugate of mapping derivative ($d\zeta*/dz'$) at i^{th} point
δ	DELI(I)	Slope of airfoil at i^{th} point
-	XNI(I)	Normalized coordinates of airfoil
	YNI(I)	at i^{th} point
V	VVI(I)	Velocity along airfoil at i^{th} point Same symbol when normalized
V_{max}	-	Maximum velocity along airfoil
$(V/V_2)^2$	V2I(I)	Normalized velocity squared at i^{th} point
$(V_{max}/V_2)^2$	PRAM	Boundary layer loading parameter S
-	IB	Number of data cards to be read during run (Fixed point integer)

–	NBE	
–	NSG	Number of values of β, σ, B_O, $\mathcal{E}$ and K
–	NBZ	
–	NEP	respectively to be read from data card
–	NAK	Fixed point integers
–	BE1	
–	SG1	Initial values of β, σ, B_O, $\mathcal{E}$ and K
–	BZ1	
–	EP1	respectively, to be read from data card
–	AK1	
–	BEI	
–	SGI	Increments of β, σ, B_O, $\mathcal{E}$ and K
–	BZI	
–	EBI	respectively, to be read from data card
–	AKI	
–	NOPR	Print mode control. Any positive fixed point integer supresses print out of results in near circle and circle plane, leaving only final cascade data.
–	NEXPR	Print mode control. Any positive fixed point integer prints detailed auxiliary information on all iteration processes.
β	BEJ	Mean flow angle, degrees
β	BE	Mean flow angle, radians
σ	SGK	Equivalent flat plate solidity
φ_B	PHEB	Velocity potential at stagnation point B
$\dfrac{dr}{d\sigma}_{K-1}$	DRUP	Slope of r vs. σ curve at previous point
$\dfrac{d\lambda}{d\sigma}_{K-1}$	DALP	Slope of λ vs. σ curve at previous point
r_B	RU,RUP,RB	Radius at stagnation point B
λ_B	ALU,ALP,ALB,	Angle coordinate at point B

R_1, R_2	R1,R2	Real functions derived from real and imaginary parts of complex transformation functions
J_1, J_2	AJ1,AJ2	
$\dfrac{d^2w}{dz^2}$	W2Z	Second derivatives of the complex potential
$\dfrac{d^2w}{d\mathcal{S}}$	W2T	
φ	PH,PHE	Velocity potential
φ_i	PHN	Velocity potential at i^{th} point
i	I,AI	Index i in fixed and floating point respectively
-	IT	Iteration count for calculation of
-	ITS	stagnation point, data points on near
-	IT3	circle, constants of circle and data
-	IT4	points on circle, respectively.
P	POWER	Exponent in initial approximation for $\triangle T$
$\triangle T$	DET	Parameter which fixes location of singularities in circle plane
φ_B	PHP	Slope of φ_B vs. T curve
-	DETNU	New estimate of $\triangle T$
θ	TE	Angle in circle plane
θ_{n+1}	TENU	New estimate of θ
θ_{n-1}	TEOLD	Old estimate of θ
	A2,A3	Various intermediate quantities as
	B2,B3	required temporarily, Some symbol may
	C2,C3,	have different meanings in different
	etc.	parts of the program
B_o	BZL	Turning parameter
γ	TAU	Angular shift in stagnation point in circle plane due to circulation

c	CHORD	Chord of airfoil
c/S	SOLID	Solidity of cascade
-	A2,RER3	Relative residual error at conclusion of various iteration processes
$\varphi - \varphi_1$	DPH	Residual error for φ in circle plane
V_Θ	VTE	Velocity in circle plane. Same as VTI(I), but not an array
-	SHIFT SIDE	Counters which increase if iteration "jumps" from upper to lower surface or vice versa. Should be zero

Sub- scripts	Post- scripts	
A	A	Front stagnation point. Zero circulation
B	B	Aft stagnation point. Zero circulation
L	L	Front stagnation point, circulation B_0
T	T	Aft stagnation point, circulation B_0
P	P	Front singularity of mapping function
Q	Q	Aft singularity of mapping function
O	O	Initial origin of coordinates
Z	Z	Shifted origin of coordinates
-	D	Degrees
Super- script	P	Indicates shifted axes

1.0 Introduction

This study is an extension of a line of investigation originally conducted by Professor Theodore H. Gawain of the U. S. Naval Postgraduate School. The original investigation, sponsored by the Aerojet General Corporation, was specifically aimed at increasing the pressure rise per stage of axial flow pumps. The intended application was to reduce the size of propellant pumps for large liquid fuel rockets. The requirements were for maximum pressure rise per stage, regardless of efficiency. This, in turn, demanded positive and accurate control of the pressure distribution around each blade, with particular emphasis on the adverse pressure gradient experienced by the boundary layer.

Flow of a real fluid through an axial flow compressor or pump involves some formidable problems. Besides the effects of viscosity and turbulence; tip losses, centrifugal force fields, and other effects complicate the problem considerably. As is usually the case in engineering however, a simplification of the problem may yield useful results. If the stream surfaces of the flow are assumed to be concentric cylinders, then a cylindrical cross section of the flow may be represented by an infinite linear cascade with two-dimensional flow. If all velocities are considered relative to the blade row, then the solution for the rotor and the stator have identical mathematical form. Following the usual aerodynamic practice, viscosity may be neglected outside the boundary layer. This

1

leaves only turbulence as a factor preventing the use of potential flow considerations. In order to use the powerful analytic methods of potential flow, turbulence has been neglected. This does not mean however, that the data presented is invalid. Actually, the potential flow assumption is used to obtain the pressure distribution only. The relation between pressure distribution and separation was obtained from experimental data from actual turbomachines, and must therefore include the effects of turbulence.

From the foregoing considerations, it may be seen that the study of cascade design has application to the whole field of axial flow turbomachinery. The problem of cascade design is much more difficult than the problem of isolated airfoil design. In the early days of airfoil design, much experimental data was obtained on a bewildering variety of shapes. However, there was no reliable method of predicting the performance of an airfoil before it was tested. It was only after the NACA (now NASA) discovered how airfoil performance depended on shape, specifically on thickness, camber and fairing distribution, that any real progress was made in the field of airfoil design.

The present state of the field of cascade design is that there is a large volume of experimental data available on a bewildering variety of cascades. Many efforts have been made to extrapolate the theory of isolated airfoils so that it will apply to cascades. However, at present there is no reliable

theory which covers the field of cascade performance in the way that NASA's theory covers the field of airfoil performance. The parameters of thickness, camber, and fairing distribution are still involved, plus a few more. The relations and interactions between these parameters are so complex, that it is very difficult to consider any aspect of cascade design separately.

When considering cascades as complete entities, the inter action effects are all present, and need not be corrected for. However, experimental efforts in this direction have been necessarily limited in scope, due to the effort and expense involved in constructing and testing large numbers of cascades. Theoretical methods, such as the one outlined in this investigation, provide the means of considering complete cascades over a wide range of design parameters. This study was undertaken from the standpoint of discovering areas of possible improvement in compressor performance.

Most of the efforts of the NASA in the field of compresor design have been for maximum efficiency with moderate output. In some cases, it may be required to attain maximum output, with perhaps moderate efficiency. The gains to be expected from these considerations are not of large order however, as a cascade develops its best efficiency not far from the point of stalling the blades.

The basic problem, then, is composed of two parts. First it is necessary to devise a method for generating blade shapes

with the corresponding pressure distributions. For this purpose, the powerful methods of complex variables and conformal transformations are utilized. The method developed by Professor Gawain generates infinite cascades of airfoil shapes, based on five arbitrary parameters. Generally, the transformations are similar to the Joukowski transformations with additional requirements.

The second part of the problem is to establish a correlation between the pressure distribution around each blade and the occurence of separation. This problem must, of course, depend heavily on experimental data. Fortunately, work has been done in this area and some practical working limits have been established. See Reference 1. Based on this data, the simple parameter $(V_{max}/V_2)^2$ has been chosen as an indication of the tendency toward separation.

The author wishes to express his sincere appreciation to Professor Theodore H. Gawain of the U. S. Naval Postgraduate School for his assistance, guidance, and encouragement during the course of this investigation.

2.0 The Method of Cascade Design

2.1 Introduction

Methods of designing airfoils by purely mathematical means have been known since the early days of aviation. Joukowski was the most notable pioneer in this field. He, and others, noted the possibility of designing cascades of airfoils by similar methods. Since the early applications of cascade design were to multi-winged airplanes, not much work was done in this field. As pointed out earlier, the application to turbomachinery makes this field of considerable interest today.

In considering the flow through cascades, the shape and position of any individual blade will affect the flow around that blade. In addition, the shape and position of all the other blades will also affect the flow around that same blade at the same time. Therefore, more parameters must be used in cascade design than are used in isolated airfoil design. In addition to blade shape, the relation of the blades to each other, and their relation to the flow must all be described. The method developed by Professor Gawain uses five independent parameters to describe an individual cascade.

The solution for blade shape and velocity distribution corresponding to chosen values of the five parameters is found by using relations of potential flow and conformal mapping in three separate planes. These have been termed the near circle plane, the circle plane, and the cascade plane respectively.

5

In reading through the following sections, which describe the general method of generating cascades, reference may be made to Figure 5, which illustrates a typical contour in each of the planes referred to above. A summary of the mathematical development of the method is given in Appendix A. A more detailed analysis may be found in Reference 2.

The solution of these equations, many of which are transcendental, is an impossible task by hand calculation. The entire problem has been arranged in FORTRAN language for solution by a digital computer. The CDC 1604 computer at the U. S. Naval Postgraduate School was used for this investigation. The basic computer program, along with later modifications is included in Appendix B.

The following sections describe the general method of generating cascades from five input parameters. Each parameter is described in detail as it enters into the calculations. The parameters are:

β = Mean flow direction

B_o = Turning parameter

σ = Equivalent flat plate solidity

ε = Thickness parameter

K = Shape or symmetry parameter

2.2 The Flow Parameters

Flow through a cascade is usually described in terms of two velocities. The first velocity is that far enough up-

stream of the cascade so that local effects due to the cascade are not evident. This is called the inlet velocity, and the angle it makes with the reference axis is called β_1. Similarly, the velocity far enough downstream so that local effects have damped out is called the outlet velocity, and its angle with the reference axis is called β_2. The magnitudes of these two velocities are not independent, since the laws of continuity require that the component perpendicular to the cascade axis be equal for the two cases. This concept allows velocities to be conveniently nondimensionalized, so that only angles are important.

Figure 1 is an illustration of two typical cascades. An appropriate velocity vector diagram is shown for each. Note that only two parameters are necessary to describe the complete diagram. Instead of the angles β_1 and β_2 it was more convenient to use two different parameters. Consider the following expressions:

$$\text{Tan } \beta = \tfrac{1}{2}(\text{Tan } \beta_1 + \text{Tan } \beta_2)$$
$$B_0 = (\text{Tan } \beta_1 - \text{Tan } \beta_2)$$

The first expression defines the angle β, or mean flow direction, which is the first input parameter. The second expression defines the turning parameter B_0, which is the second input parameter. The relationship between all these quantities is shown in the diagram on Figure 1.

The starting point of the calculations is the near circle

plane. In this plane, the complex potential for a series of
doublets spaced at intervals of 2π along the y axis is com-
bined with the potential for uniform flow at the angle β with
the x axis. The velocity of this flow is set at unity, which
then becomes the reference for all the nondimensional veloci-
ties derived later. If only one doublet were used, the resul-
ting potential would describe the flow without circulation
around a single circular cylinder. In this case, with an in-
finite series of doublets along the y axis, the resulting
potential describes the flow without circulation around an
infinite series of nearly circular bodies spaced along the y
axis. These bodies are not actually circles because the pre-
sence of the infinite stack of doublets distorts the flow
around any individual doublet, such that the flow contour is
a slightly flattened circle. The amount of distortion is re-
lated to the strength of the doublets and the spacing between
them. In this case, the spacing between doublets is fixed at
2π , so doublet strength is what determines the relation
between spacing and size of the bodies in the near circle plane.

2.3 The Solidity Parameter

The strength of the doublets is fixed by the input para-
meter σ , or the equivalent flat plate solidity. This para-
meter is closely related to, but not identical with, the ordinary
solidity c/S, or the chord-pitch ratio of the blade row. The
distinction can best be illustrated by an example. Generally,

8

any row of arbitrary blades of solidity c/S may be transformed conformally into a related row of flat plate vanes. The chord-pitch ratio of the latter is then denoted by σ. It follows that if two arbitrary cascades have the same value of σ, then either may be conformally transformed into the other. But if the value of σ is different for each, then no such transformation is possible. σ then, may be regarded as a kind of generalized solidity, of perhaps deeper aerodynamic significance than simple geometric solidity.

The relation between values of σ and geometric solidity is directly influenced by blade thickness. Very thin blades have geometric solidities almost exactly equal to σ. With thicker blades, the geometric solidity is always less. The reason for this may be illustrated by examples of two extremes. If a contour in the near circle plane is transformed conformally into a flat plate, the chord length of the flat plate will be nearly twice the diameter of the original contour. However, if no transformation is made at all, an "airfoil" of 100% thickness results, whose chord length is equal to the diameter. Both cascades would have the same value of σ, but the geometric solidity of the latter case would be half that of the former. Between these two extremes, finite thickness airfoils in cascade have solidities less than σ.

2.4 The Turning Parameter

The turning parameter, B_0, is a measure of the change in

9

direction of the flow passing through the blade row. It is actually a nondimensional form of the downwash velocity induced by the blades. There is a very simple relation between B_0 and the circulation around each blade. In fact, for a constant mean flow angle, this relation is a simple direct proportion. This convenient state of affairs is the reason why the two flow parameters were expressed in their present form.

In isolated airfoil theory, the method of introducing lift or circulation on an airfoil, is to add to the complex potential, a term representing a vortex of suitable strength. However, mere addition of a vortex will produce a distortion in the contours in the near circle plane, since these contours are not exactly circles. In addition, an infinite stack of vortices is necessary to produce circulation around each of the blades in the cascade. To avoid these resulting undesirable perturbations in what will ultimately become the airfoil shape, and indirect method of adding circulation is used.

In this method, a transformation is made from the near circle plane to the circle plane. An equation is developed which transforms the flow in the near circle plane into the flow around a perfect circle, centered on the origin. The circulation term may then be introduced without fear of distortion. The transformation is then made back to the near circle plane. Since the same equation is used to transform both ways, the original flow contour remains unchanged; however, the velocities at each point are now different, due to the circu-

lation.

2.5 The Blade Shape Parameters

The final transformation is from the near circle plane
to the cascade plane. This is done by the Joukowski method
of shifting the axes slightly in such a way that the flow con-
tour transforms into an airfoil shape. Two arbitrary para-
meters were chosen to control the blade shape. One of these
is called the thickness parameter, and is given the symbol $\mathcal{E}$.
This quantity is generally related to the thickness, and also
to nose curvature, but not in any fixed relationship. Large
values of $\mathcal{E}$ produce thick airfoils, and small values produce
thin airfoils. Figure 2 is an illustration of several airfoils,
showing the effect of $\mathcal{E}$. The limiting value of 0 for $\mathcal{E}$ does
not however produce an airfoil of zero thickness. Due to the
slight distortion of the contours in the near circle plane,
$\mathcal{E} = 0$ may produce the mathematically significant, but physi-
cally useless case where the "lower" surface of the airfoil
crosses through the "upper" surface. $\mathcal{E}$ then, can be small but
not zero, and the airfoils produced can be thin but not of zero
thickness.

The other parameter is the shape or symmetry parameter K.
The effect of variations in K may be seen in Figure 3. Gener-
ally, K=0 produces a blunt leading edge, and cusped trailing
edge similar to a Joukowski airfoil. K=1 will produce a sym-
metrical shape which is generally a cambered ellipse. As K

11

increases from zero to one, the point of maximum thickness moves from the quarter chord to the half chord point, and the trailing edge rounds off. Values of K larger than one will produce airfoils facing the wrong way (Trailing edge into the flow) and hence must not be used.

2.6 Stagnation Points

During the transformations made in this analysis, the stagnation points serve as reference points to locate the relation of the contours in the various planes. For this reason there is always a stagnation point at the leading and the trailing edge. Having a stagnation point at the leading edge is sometimes called the Theodorsen condition. This means that in all the cascades developed by this method, the airfoils are operating at the ideal angle of attack. Variations in lift then, are achieved by variations in the camber of the blades. Figure 1 graphically illustrates this fact. Two typical cascades are drawn, with the principal variation being in turning parameter, B_o. The values of $\mathcal{C}$ were adjusted to give the same blade thickness. The difference in camber may be clearly seen.

The condition of a stagnation point at the trailing edge is called the Kutta condition. This fact has particular significance when considering the blade shapes where K=1. As pointed out previously, these shapes are generally cambered ellipses. It is a well known fact that flow around an ellipse

of a given thickness ratio produces a lower velocity peak than
the flow around any other shape of the same thickness ratio.
This class of blades then should exhibit the lowest loading
attainable for any possible fairing shape. Of course, any
attempt to duplicate this fairing shape in an actual cascade
is doomed to failure because of the rounded trailing edge.
However, this case still has significance in two respects.
First, the performance of a cambered ellipse, with the Kutta
condition mathematically imposed, represents a useful limiting
case of performance due to fairing shape. Secondly, a blade
similar to this, with modifications to produce a sharp trail-
ing edge, would have very nearly the same performance. The
critical area of flow near the leading edge would not be af-
fected much by modifications at the rear of the airfoil.

Figure 4 is a plot of the pressure distribution around
the airfoils of Figure 3. The above premise is verified, as
the negative pressure peak can be seen to decrease as the
value of K is increased. Note that the pressure distribution
aft of the peak is essentially linear to the trailing edge.
Reference 3, p. 354 states that this type of pressure distri-
bution is typical of decelerating cascades. Note also that
the slope of this line becomes less as K is increased, indi-
cating a less adverse pressure gradient in the boundary layer.

3.0 Prediction of Separation

3.1 Pressure Gradient

The phenomenon which ultimately limits the attainable
pressure rise of a cascade is separation. Flow separation
occurs when flow in a boundary layer experiences an adverse
(positive) pressure gradient. This adverse gradient tends to
decrease the velocities in the boundary layer. Ultimately,
the point is reached where the velocities close to the surface
have been reduced to zero. At this point, flow separation
occurs. Beyond this point, some velocities become negative,
and a region of reverse flow exists. The resultant effects
cause high drag and loss of circulation around each blade
element. Many experiments have verified that any adverse
pressure gradient, however small, will cause separation if it
acts long enough. The concept of a gradient and the distance
over which it acts, leads one naturally to suspect pressure
difference as a significant parameter in predicting separation.
The gradient, integrated over the distance is mathematically
equal to the difference in pressure. It was previously shown,
furthermore, that the pressure distribution over typical air-
foils in this system is approximately linear aft of the nega-
tive pressure peak.

3.2 Velocity Considerations

From another point of view, one might examine the velo-
cities of flow through a cascade. From the inlet velocity

described previously, velocity is brought to zero at the front stagnation point, accelerated to a local maximum somewhere on the surface of the blades, reduced toward zero at the trailing edge, and finally settles down to the outlet velocity far behind the cascade. Besides the inlet and outlet velocities, only one other velocity is really significant, and that is the local maximum, V_{max}. From these three quantities, only two independent dimensionless parameters may be constructed. If the inlet velocity and V_{max} were used, this parameter would be related to the flow around the forward part of the airfoil. Since this flow involves a negative pressure gradient, it is probably not very significant with respect to separation. Similarly, the quantities V_{max} and the outlet velocity, called V_2, are related to the flow around the rear part of the airfoil, which involves a positive pressure gradient. These two parameters then, combined in some dimensionless manner, should act as an indicator for the tendency toward separation.

3.3 Diffusion Factors

From its many experimental studies of flow through cascades, the NASA has arrived at essentially the same conclusion. They have used several dimensionless combinations of V_{max} and V_2 to define blade loading limits. One of these is the "Local Diffusion Factor" which is:

$$D_1 = \frac{(V_{max} - V_2)}{V_{max}}$$

This factor is described in Reference 1 and supporting data indicates that separation is likely to occur for values of D_1 greater than 0.5.

Since the velocity distribution around the blades must be known to find values of D_1 , it is necessary to use experimental data, or an analytical treatment such as the one described in this investigation. To get around this difficulty, the NASA also defines an approximation, D, which may be obtained from more easily determined quantities. D, is called the "Diffusion Factor" and is given by:

$$D = 1 - \frac{\cos \beta_1}{\cos \beta_2} + \frac{\cos \beta_1}{2 \, \sigma/s} (\tan \beta 1 - \tan \beta 2)$$

It is seen that this quantity can be determined from the inlet and outlet velocities, and the solidity of the blade row. The supporting data indicates that separation is likely to occur for values of D greater than 0.6.

Since the methods used in this investigation furnish all of the flow quantities described above, as well as the complete velocity distribution around each blade, the opportunity to compare the two NASA parameters is presented. As will be described later, the correlation between these two parameters is not too good for the solidities considered here.

16

3.4 The Boundary Layer Loading Parameter

From the above development, it may be seen that the parameter to indicate separation should involve the pressure ratio across the rear part of the airfoil, and be some dimensionless combination of the quantities V_2 and V_{max}. The NASA has indicated that most compressors operate in the range where Reynolds number effects are insignificant. Therefore, it is felt that no particular inaccuracies result from omitting consideration of Reynolds number.

In order to avoid using one parameter for pressure distribution, and another for the tendency toward separation, the quantity S was selected where:

$$S = (V_{max}/V_2)^2$$

This quantity is referred to as the boundary layer loading parameter, and is quite versatile in application. It is directly related to the pressure coefficient, and in fact only differs from that quantity by unity. S also has a constant functional relationship with the NASA parameter D_1. The value $S = 4.25$ corresponds to the value of D_1 of 0.5, and has been selected as the limit loading in the boundary layer for blades in this investigation.

17

4.0 Results and Discussion

Theory and experiment both point toward increasing solidity as the method of obtaining increased pressure rise per stage. As solidity is increased, the lift coefficient on each blade is decreased, and hence the loading on the boundary layer is decreased also. However, as the solidity is increased, there is an adverse effect due to the blockage caused by the finite thickness of the blades plus the boundary layer. Finally, the point is reached where the beneficial effects of decreased blade loading are just counterbalanced by the adverse effects of blockage. The quantitive determination of this point was one of the major objectives of this investigation.

4.1 Organization and Scope

Since actual cascades are designed on the basis of blade thickness and geometric solidity, it was felt that the results of this investigation ought to be organized on this basis, rather than on the basis of the mathematical parameters $\mathcal{E}$ and σ. The value of blade thickness is not directly predictable from the input parameter $\mathcal{E}$. Therefore, the basic computer program was modified to use an iterative scheme to achieve the desired values of blade thickness. Details are given in Appendix B, which describes the basic computer program and the modifications. Seven blade thicknesses were selected to cover the field of possible blades. These ranged from the limiting

18

case of extremely thin blades to 24% thickness blades in four percent increments.

It was decided to conduct this investigation using only one value of average flow angle β. This value was chosen to be 45°, which was a somewhat arbitrary decision, but not without some sound theoretical basis. It is stated in Reference 4 that maximum efficiency may be obtained when the average flow angle is near 45°, and many compressors are built accordingly.

In spite of reducing the parameters to four by the above decision, over 1470 separate cascades were generated and analyzed for this investigation. Additional parameters could have been introduced to give more control over the blade shape, but they would have greatly magnified the problem. As the data will show, additional blade shape parameters would not have affected the significance of the results very much.

4.2 Series 1 Plots

The first plots of data from the computer run were made of boundary layer loading vs. solidity, for airfoils of constant blade thickness. Five values of the shape parameter K were used, and data was obtained at six values of turning parameter, B_0. This meant that there were 30 graphs in series one. Figures 6 through 9 are representative graphs from this series.

It was noted with satisfaction that the curves showed a

19

pronounced minimum loading as solidity was increased. The one exception was the case of the extremely thin airfoils, for which the curve appeared to be asymptotic to some low value of loading. This is not unreasonable, since the blockage effect would be very small for this case. The case of thin airfoils then, represents a sort of limiting value for cascades. The point at which minimum loading occurred for a given thickness airfoil was called the optimum solidity.

It may be noted that while the value for loading at an optimum point could be determined with accuracy, the corresponding solidity for that point was subject to some uncertainty. Therefore, another point was introduced where the solidity could be determined with greater certainty. This was called the design point, and is defined as the point toward lower solidity where the loading equals 1.10 times the minimum value. There is further justification in this step from the fact that the basic analysis neglects boundary layer. The blockage effect of a blade plus boundary layer must be greater than the effect due to the blade alone. Therefore, the true optimum solidity must be somewhat less than the apparent optimum based on non-viscous flow. The exact relation cannot be found without a detailed analysis of the boundary layer. This simple method sidesteps this formidable problem, and is at least qualitatively in the right direction.

For the case of higher values of turning parameter and thick blades, there was some scatter in the data. Since the

data is all analytical, and should therefore be reasonably regular, some effort was made to find the source of the scatter. The relationship between the parameters σ and c/s was suspected first. Comparative plots of these two parameters however, showed that they varied in a regular fashion with blade thickness. It was then decided that the scatter was due to the fact that velocities were measured only at 40 points along the airfoil. If the true maximum velocity occurred between these finite points, then the value for boundary layer loading parameter would be in error. Remembering the fact that this error could be only on the low side was an aid in fairing the curves through the scattered points.

It was noted that the data became more regular as the value of K approached one. For these airfoils, either the flow was more regular about the nose, with no sharp peaks in velocity, or the point of maximum velocity happened to coincide more often with one of the finite points. Examination of the pressure plots of Figure 4 points toward the former as the cause. With high values of K, the pressure changes are seen to be more gradual, and of lower magnitude. Because of this, the actual maximum velocity was always close to the velocity recorded at one of the 40 points.

Figure 10 is an illustration of the effect of K in reducing the boundary layer loading for a given value of turning parameter. With all other factors equal, the loading steadily decreased as the value of K increased toward unity. Note that

the effect of K was much greater for the thick blades. For
the case of extremely thin blades, K had no effect at all,
which was not an unexpected result.

4.3   Series 2 Plots

Since the original series involved 30 graphs, some effort
was made to summarize this data. The result of this effort
was Figures 11 through 15, which collect all the data for a
particular value of K on a single page. Boundary layer load-
ing parameter and solidity are plotted along the coordinates
as before, but now the solidity is design solidity. In effect,
all the design points for a particular value of K have been
plotted. Points of constant values of turning parameter have
been connected, as have points of constant airfoil thickness.
The result is that four interdependent parameters are shown
for each point on the chart. Any chosen point then, repre-
sents a particular value of blade thickness and turning para-
meter, with the corresponding boundary layer loading and
design solidity for the cascade.

Figures 16 through 20 are plots made in exactly the same
manner, except that optimum points were used instead of design
points. It was necessary to change the scale for solidity
along the horizontal axis, since optimum points represent
higher values of solidity in every case. In addition some
difficulty was experienced with irregularity in the data.
This was due at least in part to the uncertainty in determin-

22

ing the value of solidity at the optimum point. This optimum point data was included as a limiting case, to illustrate the maximum solidities to be used when the boundary layer is negligibly thin.

The choice of solidity as a coordinate is slightly misleading. It might be inferred from this choice that solidity should be used as a design input. However, solidity was plotted in this manner purely as a convenience in transferring data from the series one graphs. In design work, the two "inputs" could be boundary layer loading, and turning parameter. The "output" information would then be blade thickness and solidity. An attempt was made to plot boundary layer loading parameter vs. turning parameter, but the resulting blade thickness and solidity lines were so nearly parallel that the information was difficult to read.

4.4 Comparison of NASA Separation Parameters

The data on the series 2 plots contains all of the information necessary to compute both NASA separation parameters. This affords an opportunity to compare these two parameters directly. The boundary layer loading parameter S, and the NASA parameter D_1 have a constant relationship such that:

$$ D_1 = 1 - \frac{1}{\gamma S} $$

Thus a D_1 equal to 0.5 corresponds to a value of S of 4.25. This value is entered as a heavy line on all series 2 plots.

23

The approximation D, is related to the parameters B, B_0, and c/S by the following relationship:

$$D = 1 - \sqrt{\frac{1 + \left(\tan\beta - \frac{B_0}{2}\right)^2}{1 + \left(\tan\beta + \frac{B_0}{2}\right)^2}} + \frac{B_0}{2\,c/S\sqrt{1 + \left(\tan\beta + \frac{B_0}{2}\right)^2}}$$

Thus, since β has been fixed at one value, each value of B_0 and c/S will result in a particular value for D. This expression for D shows that it cannot be a good approximation over a wide range of solidities, since it indicates that loading will always decrease whenever solidity is increased. It has already been demonstrated that as solidity increases beyond the optimum point, loading increases also due to the blockage effect.

Lines corresponding to a value of D=.5 and D=.6 have been plotted on Figures 11 through 20 as dashed lines. A note of caution is necessary in using the data on these figures. It must be remembered that there is really only one solidity shown on each chart, and that is the design (or optimum) solidity. The fact that solidity is shown as a variable is due solely to the fact that each combination of blade thickness and turning parameter demands a particular value of solidity at the design (or optimum) point.

If the parameter D is a true approximation for D_1, then the lines corresponding to D=.5 and D_1=.5 should be nearly the same. Examination of the figures shows that there is a

fair match for the case of optimum solidity. Generally, D gives a value of loading which is higher than D_1, but the error is only around 10%, which is not unreasonable. For the case of design solidity, there is a greater discrepancy. For very thick blades, D still indicates a value of loading higher than D_1, but this relation reverses so that for thin blades D_1 indicates the higher loading.

The data in Reference 1 states that separation is likely to occur for values of D_1 greater than .5 or for values of D greater than .6. This in itself is an indication of a mismatch between D and D_1. If the occurrence of separation is taken as the matching criterion, then the line corresponding to $D=.6$ should match the $D_1=.5$ line. For the case of optimum solidity it may be seen that the matching is very poor, where D indicates a much higher loading than D_1. At design solidity the matching is better, but D still indicates values of loading which are around 18% higher than D_1. Extrapolating this trend leads one to suspect that, for some value of solidity less than design solidity, the two parameters $D=.6$ and $D_1=.5$ would probably match quite closely. From this, it is not unreasonable to expect that the NASA obtained its experimental data from cascades whose solidity was less than the design or optimum as defined in this report. A few checks of source data for Reference 1 have verified this premise. Solidities were generally 1.0 for cascades with blade thicknesses of eight and ten percent. A check of the series 2 plots will

reveal that this is less than the design or optimum point for any fairing shape.

4.5 Comparison of Blade Thickness and Fairing Shape Effects

Figures 11 through 20 clearly show the gains that can be made in turning parameter, at no increase in loading, by using thinner blades at the corresponding higher solidities. However, it was desired to compare the effects of changes in fairing shape and blade thickness on the same chart. Figure 21 was made using the design point data, and Figure 22 was made with data from the optimum points. The value of $S = 4.25$ was selected as the best estimate of maximum permissible blade loading. The values plotted were turning parameter vs. solidity at this constant value of blade loading. This resulted in lines which represented varying blade thickness at a constant value of K. Lines of constant blade thickness were then drawn in. It is interesting to note that these lines are nearly vertical. This means that the value of design or optimum solidity for a particular blade thickness is relatively independent of blade shape. This result was not directly predictable from theory, and may prove useful in planning experimental investigations.

As blade thickness is decreased, it is clearly seen that the importance of fairing shape decreases correspondingly. When blade thickness reaches about four percent, there is almost no discernible difference due to fairing shape. To

compare the relative effects of fairing shape and thickness changes, consider the following example. Select a blade thickness of 12% with K = .010, which is a relatively poor fairing shape with a blunt nose. For this shape at the proper solidity, a turning parameter of .74 is possible without separation. If K = .990 the shape is nearly the best possible.

Making this change increases the permissible turning parameter to .83, or a 12% improvement. This same improvement could be obtained with the original shape by decreasing the thickness to a little less than 8% and increasing the solidity slightly. If the blades could be decreased to 4%, with the corresponding increase in solidity, the turning parameter could be increased to .92 without changing the loading. This is a 24% improvement, or double the best improvement that could be obtained by fairing shape changes alone. As a limiting value, if the blades could be made infinitesmally thin, the increase in turning parameter could be as high as 50%.

It must be remembered that these performance figures are for cascades operating only at the ideal angle of attack. It may well be that these increases in peak performance are attained with some sacrifices in flexibility. This would be of no consequence in a constant output device, but for general application, the problem of operating off-design must be considered. The analytical method described in this study can be modified to consider the case of operating at angles of attack other than the ideal. This matter is discussed more fully in the section on suggestions for further work.

27

5.0 Conclusions

It is concluded that the method of generating cascades as described in this report is a workable one, and provides useful results. Cascades are generated as complete entities, which eliminates the need for separating the effects of the various design parameters. Use of a high speed digital computer means that large numbers of cascades can be generated and analyzed quickly. This allows exploration over a wide range of design parameters.

Solidity in experimental cascades has often been arbitrary. This investigation has revealed that the matter of solidity is of paramount importance. For any combination of fairing shape, thickness and camber, there is a particular value of solidity which will result in the lowest loading of the boundary layer. This loading can increase quite rapidly as the solidity is varied from the proper value.

Data obtained in this investigation has yielded the unexpected result that the optimum value of solidity referred to above is relatively independent of the fairing shape of the blades. An important application of this result will be in planning experimental investigations of cascade performance. The actual values of solidity given in this report may be used, with the probability that they will be close to the optimum values for any sort of physical blade shape.

Three parameters intended as indicators of the tendency toward flow separation were compared in this report. As a

28

result of this comparison, it is concluded that the parameter
S, as defined in this report, is a useful indicator in this
respect. It is further concluded that the value S = 4.25 is
an acceptable design limit, which is as consistent with NASA
data as this data is consistent with itself.

With respect to the problem of increasing the performance
of airfoils in cascades, it is concluded that the matter of
blade thickness is of much greater importance than the fairing
shape. The example was given of a cascade with blades of 12%
thickness. Possible increases in turning parameter for this
cascade due to improvements in fairing shape were shown to be
on the order of 12%. Increases in turning parameter produced
by decreasing the blade thickness to 4% with a corresponding
increase in solidity, were shown to be 24%, or twice the pre-
vious amount. The absolute limit of performance increase by
this method would be given by the case of negligibly thin
blades. For this case, the total increase in turning parameter
would be 50%.

It was pointed out in this study that increasing the
performance of cascades by using thinner blades and higher
solidities would probably reduce the flexibility of performance.
The effects of operating off-design were not a part of this
study since the method of generating the cascades produced
airfoils operating only at the ideal angle of attack. It was
stated that modifications could be made in the method to con-
sider the off-design case, but this was not done due to time
limitations.

6.0 Suggestions for Future Work

This investigation represents only a beginning in the field of theoretical design. With the basic method and computer programs available, it should be a simple matter to extend the scope of investigations similar to this one. Investigations ought to be conducted for a number of average flow angles, so as to cover the whole range of possibilities in cascade design. Reference 2 for example, has some work on an average flow angle of zero, which represents the special case of an impulse turbine. There is no reason to prevent considering negative average flow angles either. This would be the case of turbines rather than compressors, but the same method and computer program would apply.

One might suppose that since the flow is accelerated through a turbine, the boundary layer experiences a negative pressure gradient and separation is not a problem. This is not exactly true, however. There are actually two pressure differences to consider in flow through a cascade. One is the effect perpendicular to the stream, which is a result of the lift being developed by each blade. The other is the longitudinal effect parallel to the stream which is the result of differences in pressure from the front to the rear of the blade row. Flow separation depends on the combination of these two effects. Thus, in decelerating cascades, the longitudinal effect reduces the allowable lift from each blade. In turbines, the longitudinal effect increases the allowable lift.

If the lift is increased enough to overcome the aid of the
longitudinal effect, flow separation will still occur. A
series of studies of this matter could establish the exact
relation between these two gradients and the occurrence of
separation.

The analytical methods of this report would be a help in
studying the occurrence of separation through solution of the
boundary layer equations. The detailed pressure distributions
provided by the computer at least open an avenue toward solu-
tion of the boundary layer equations by direct integration.

In any future work, it would be convenient to consider
the velocity at more points near the leading edge of the blades.
This would allow more accurate determination of the actual
maximum velocity, and should eliminate some of the scatter
found in the data for this investigation. The necessary modi-
fications to the computer program are not difficult, and only
lack of time prevented their incorporation in this investiga-
tion.

Another area of investigation would be a change in the
basic transformation which would allow a finite angle at the
trailing edge of the blades. This would make the transforma-
tions similar to the Karmann-Trefftz transformations then,
rather than the Joukowski. Eliminating the cusp or radius at
the trailing edge then, would perhaps yield blade shapes which
would be more physically useful. As pointed out earlier, some
of the blade shapes developed in this investigation, while

mathematically useful, were physically poor because of the rounded trailing edge. These improved transformations would be particularly useful in the case of symmetrical impulse blading, where a finite angle is desired at both the leading and the trailing edge.

As mentioned previously, it would be interesting and per-haps useful to consider the off-design case, where the blades are operating at some angle of attack other than the ideal. In principle, the method would be to generate the airfoils, then go back to the original complex potential and change the average flow angle. Keeping the same transformations would preserve the blade shape, but the circulation would have to be adjusted to keep the Kutta condition. The idea seems simple enough, but no doubt there will be many difficulties with the details.

Still further work could be done in investigating other shapes for the camber line of the blades. Generally, the camber line for the blades developed in this investigation was the slightly flattened arc of a circle. The generation of other camber lines involves the expression for the flow poten-tial in the near circle plane. In this plane, a single doub-let generates the flow contour which transforms into one of the blades of the cascade. If instead, a series of doublets were used; by varying the strength and distribution of these doublets, great control could be exercised over the camber line and blade shape of the airfoils. The ultimate in this

direction would be where the input is a desired pressure
distribution, with the proper camber and blade shape being
automatically produced. The resultant family of cascades
would be as important a milestone to cascade design as the
NASA 6-series airfoils were to isolated airfoil design.

BIBLIOGRAPHY

Ref. 1:   Anon. "Aerodynamic Design of Axial-Flow Compressors",
          Vol II, NACA Research Memorandum E56B03a, 1956

Ref. 2:   Gawain, T. H., "Design and Performance Analysis of
          Cascades of Blades by Digital Computer", Report
          AGLR Number 5, July, 1962

Ref. 3:   Vavra, M. H., Aero-Thermodynamics and Flow in Turbo-
          machines. New York: John Wiley & Sons, Inc., 1960

Ref. 4:   Shepherd, D. G., Principles of Turbomachinery. New
          York: The MacMillan Company, 1956

Material used as background but not referred to specifically
in the text.

          Streeter, V. L., Fluid Dynamics. New York: McGraw-
          Hill Book Co., Inc. 1948

          Prandtl, L. and Tietjens, O. G., Fundamentals of
          Hydro- and Aeromechanics. New York: McGraw-Hill
          Book Co. 1934

          Pope, Alan, Basic Wing and Airfoil Theory. New York:
          McGraw-Hill Book Co. 1951

TYPICAL CASCADES, SHOWING THE EFFECT OF TURNING PARAMETER, B_o

$B_o = .50$

$B_o = 1.10$

OTHER PARAMETERS

$\beta = 45°$

$K = .255$

$\epsilon = .143$

SOLIDITY = .944

THICKNESS = .120

$\sigma = 1.050$

STAGGER ANGLE

$41.07°$

V_1

V_2

$B°V_1$

β

ρ

β_2

STAGGER ANGLE

$35.27°$

OTHER PARAMETERS

$\beta = 45°$

$K = .255$

$\epsilon = .122$

SOLIDITY = .913

THICKNESS = .120

$\sigma = 1.050$

SUCTION SIDE

PRESSURE SIDE

$\left(\frac{V}{V_2}\right)^2$

PRESSURE DISTRIBUTION

$\left(\frac{V}{V_2}\right)^2$
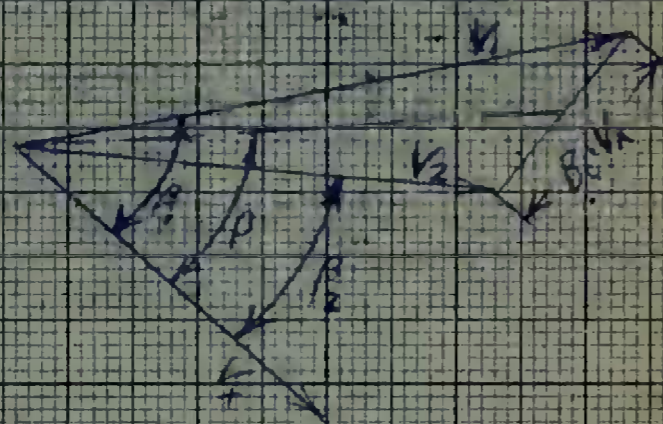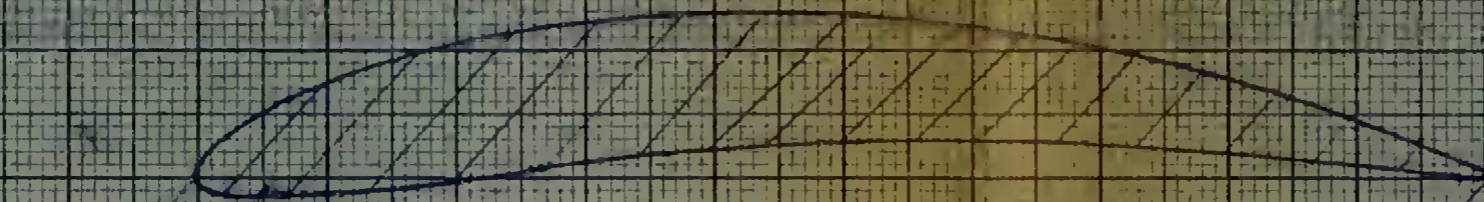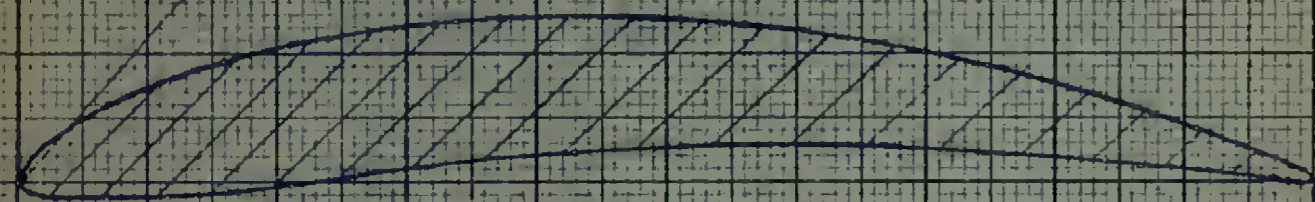
SUCTION SIDE

PRESSURE SIDE

PRESSURE DISTRIBUTION

$\mathcal{E}$ = .050   Thickness = .044

$\mathcal{E}$ = .150   Thickness = .125

$\mathcal{E}$ = .250   Thickness = .206
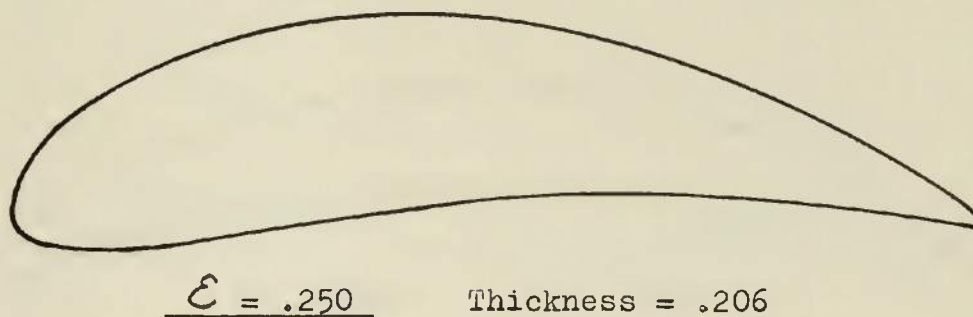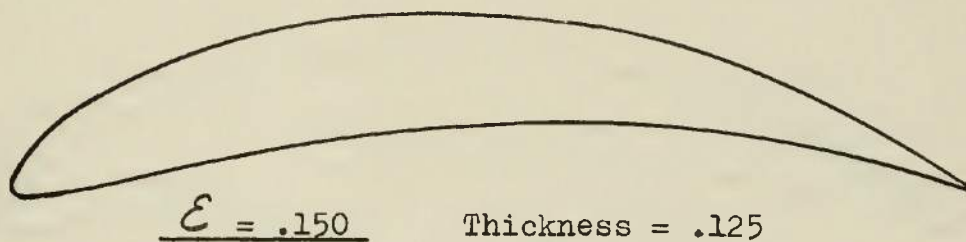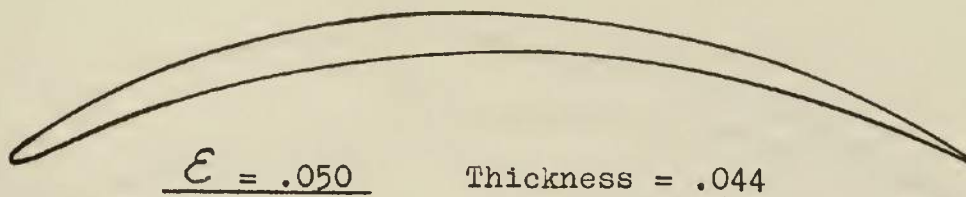
Beta = 45° B_o = 1.00 σ = 1.500   K = .250

Figure 2.

The Effect of Parameter $\mathcal{E}$ on Blade Shape

36
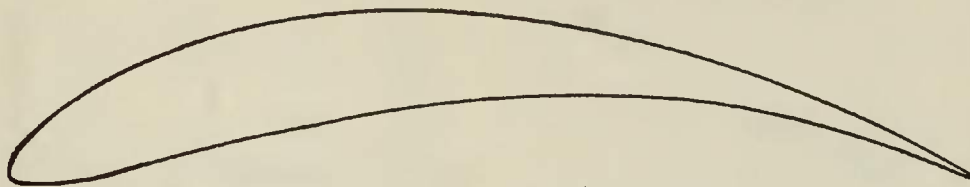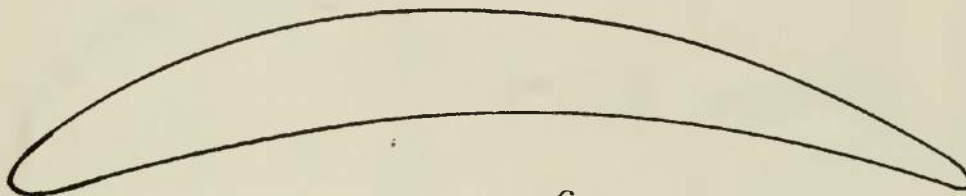
K = .010 $\mathcal{E}$ = .150

K = .500 $\mathcal{E}$ = .118
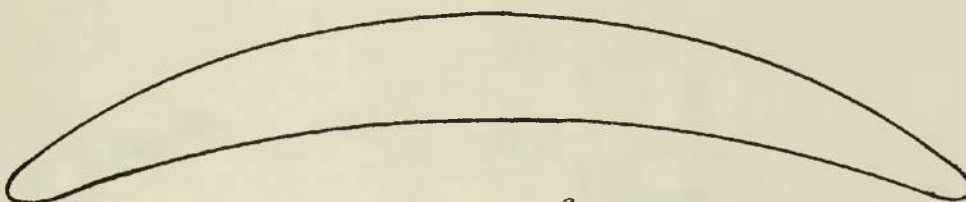
K = .990 $\mathcal{E}$ = .095

Beta = 45° B_o = .80 σ = 1.050   Thickness=.118

Figure 3.

The Effect of Parameter K on Blade Shape

The Effect of Parameter K on Pressure Distribution

K = .010

$\mathcal{E}$ = .150

Suction Side

Pressure Side

$\left(\dfrac{V}{V_2}\right)^2$

.1   .2   .3   .4   .5   .6   .7   .8   .9

K = .500

$\mathcal{E}$ = .118

Suction Side

Pressure Side

$\left(\dfrac{V}{V_2}\right)^2$

.1   .2   .3   .4   .5   .6   .7   .8   .9

= .990

= .095

Suction Side

Pressure Side

$\left(\dfrac{V}{V_2}\right)^2$

x/c
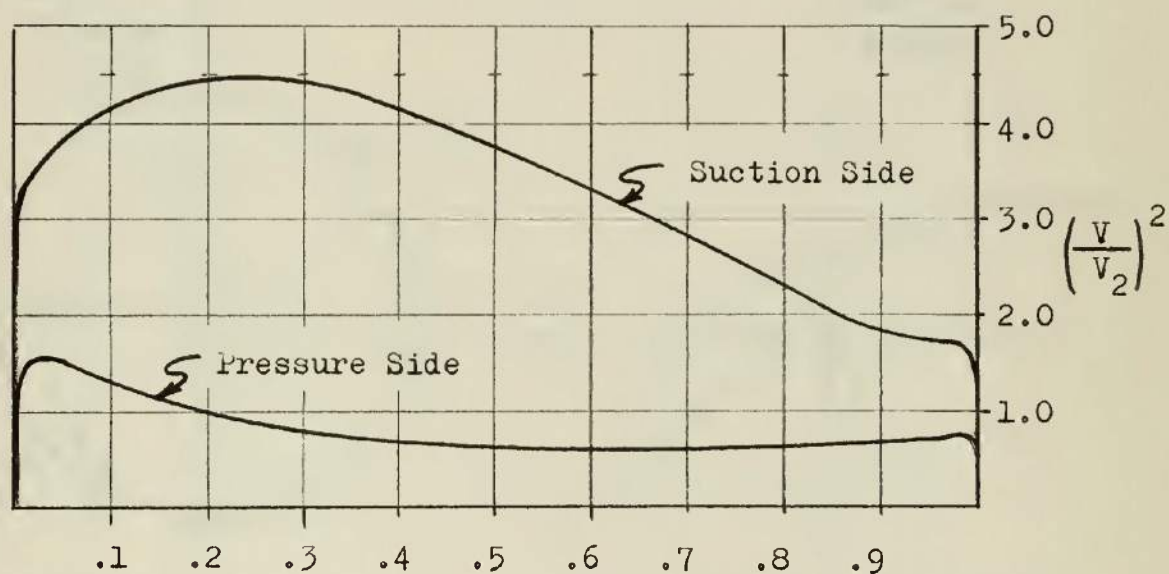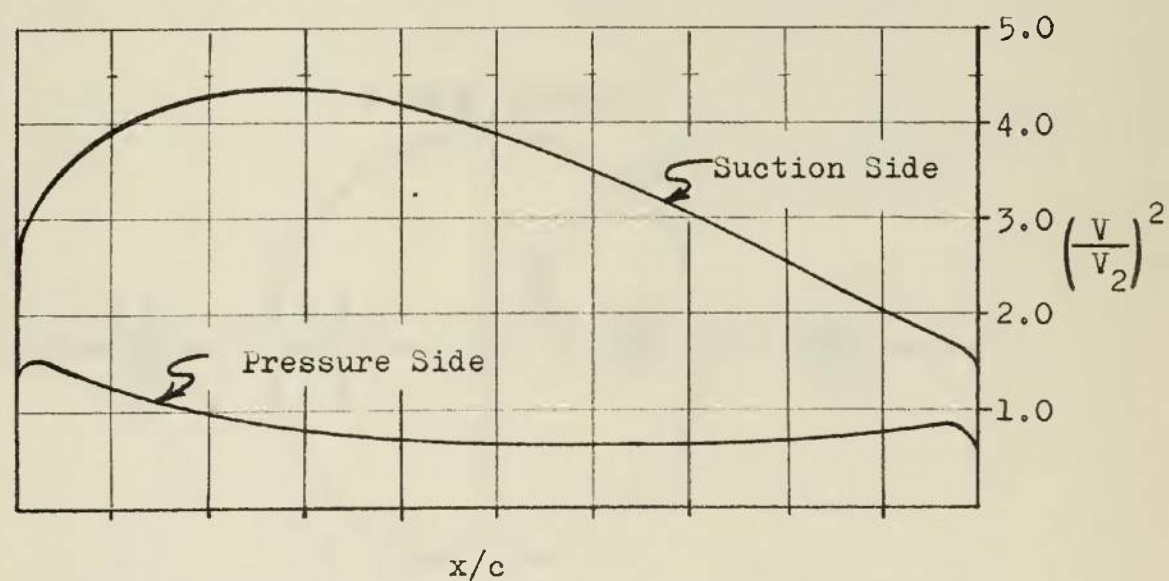
Beta = 45°   B$_o$= .80 σ = 1.050   Thickness = .118

Figure 4.

38
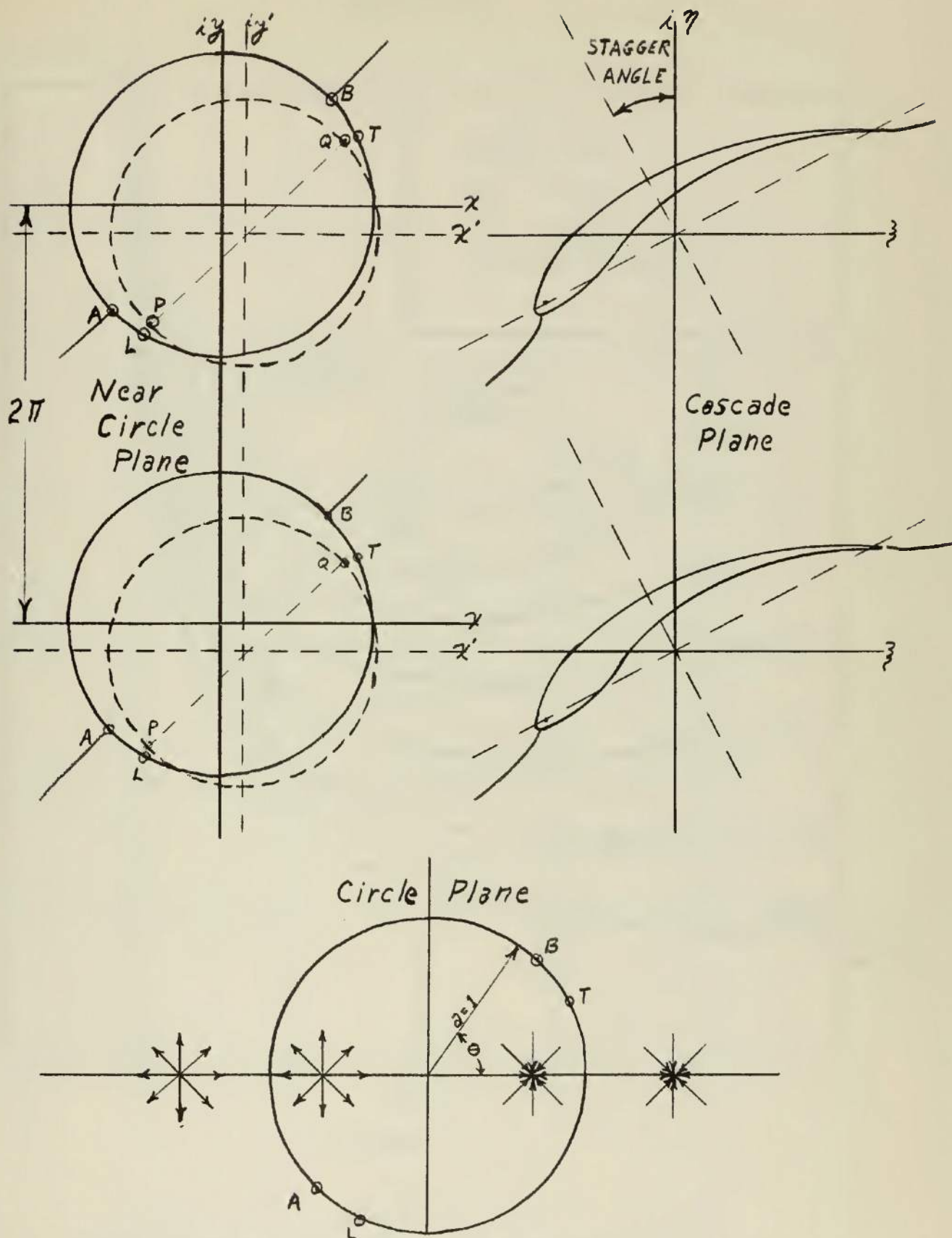
Figure 5. Examples of Contours in Each Plane

39
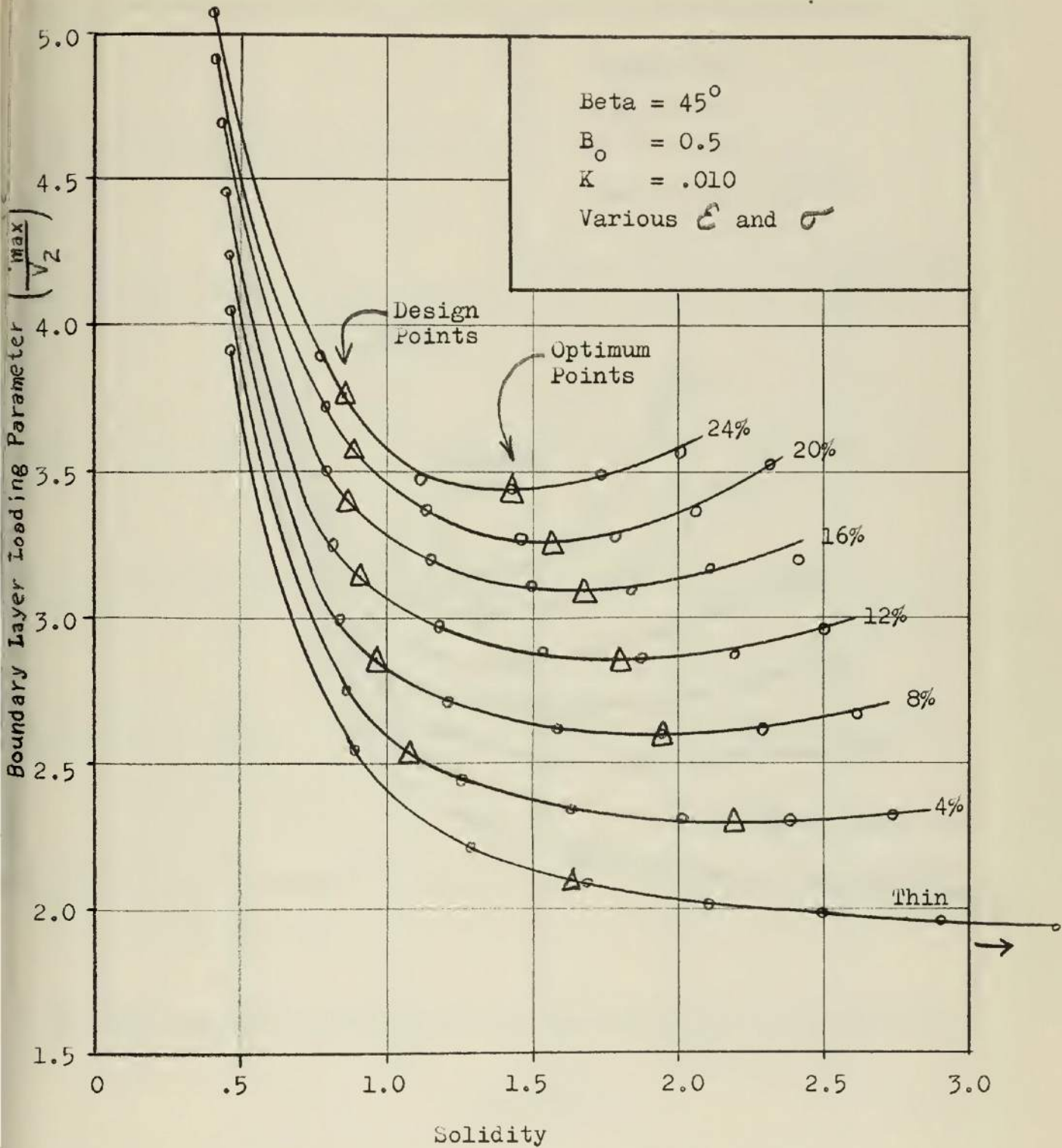
Figure 6.

Boundary Layer Loading Parameter vs. Solidity

For Constant Thickness Airfoils

40
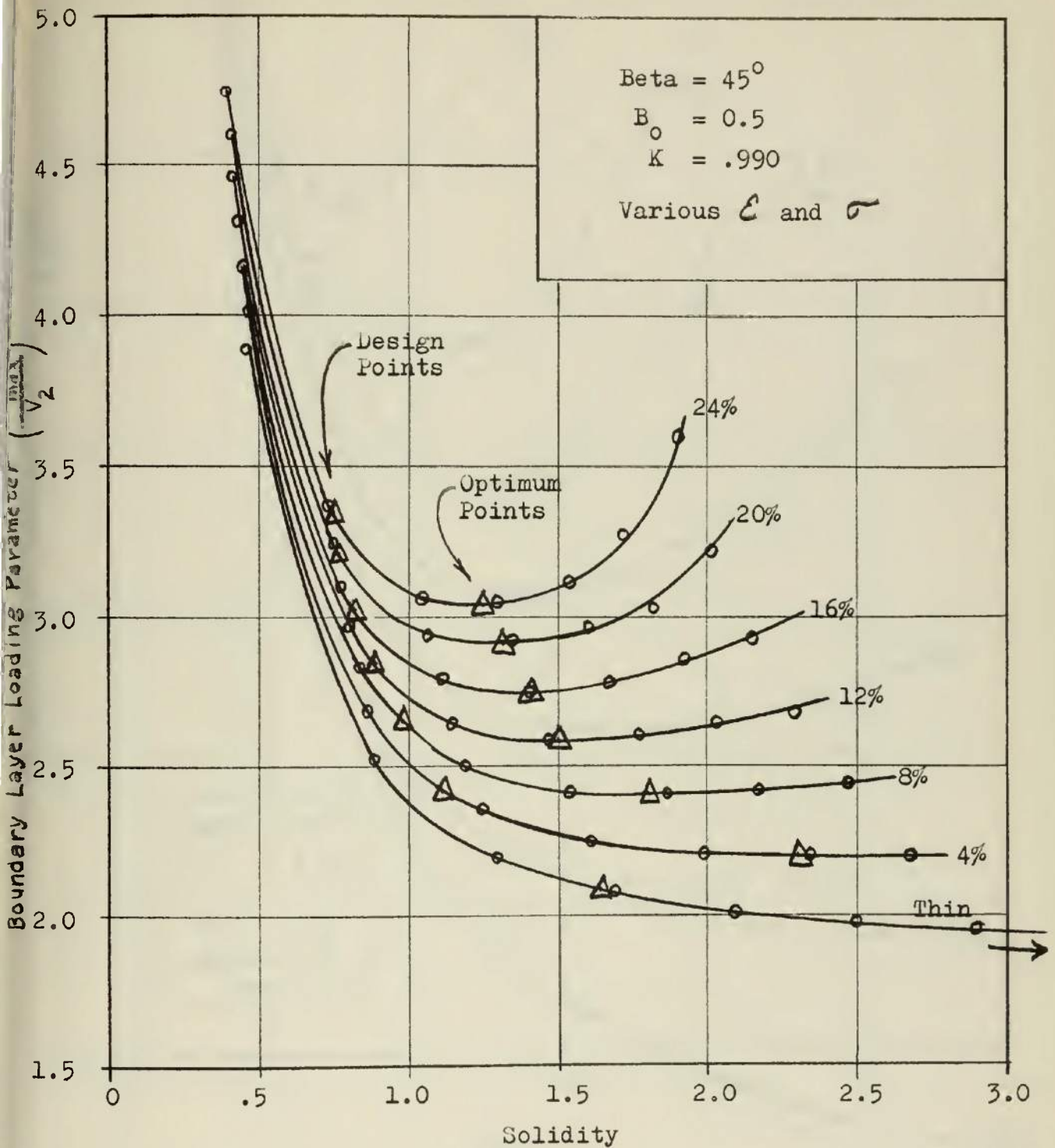
Figure 7.

Boundary Layer Loading Parameter vs. Solidity

For Constant Thickness Airfoils

41
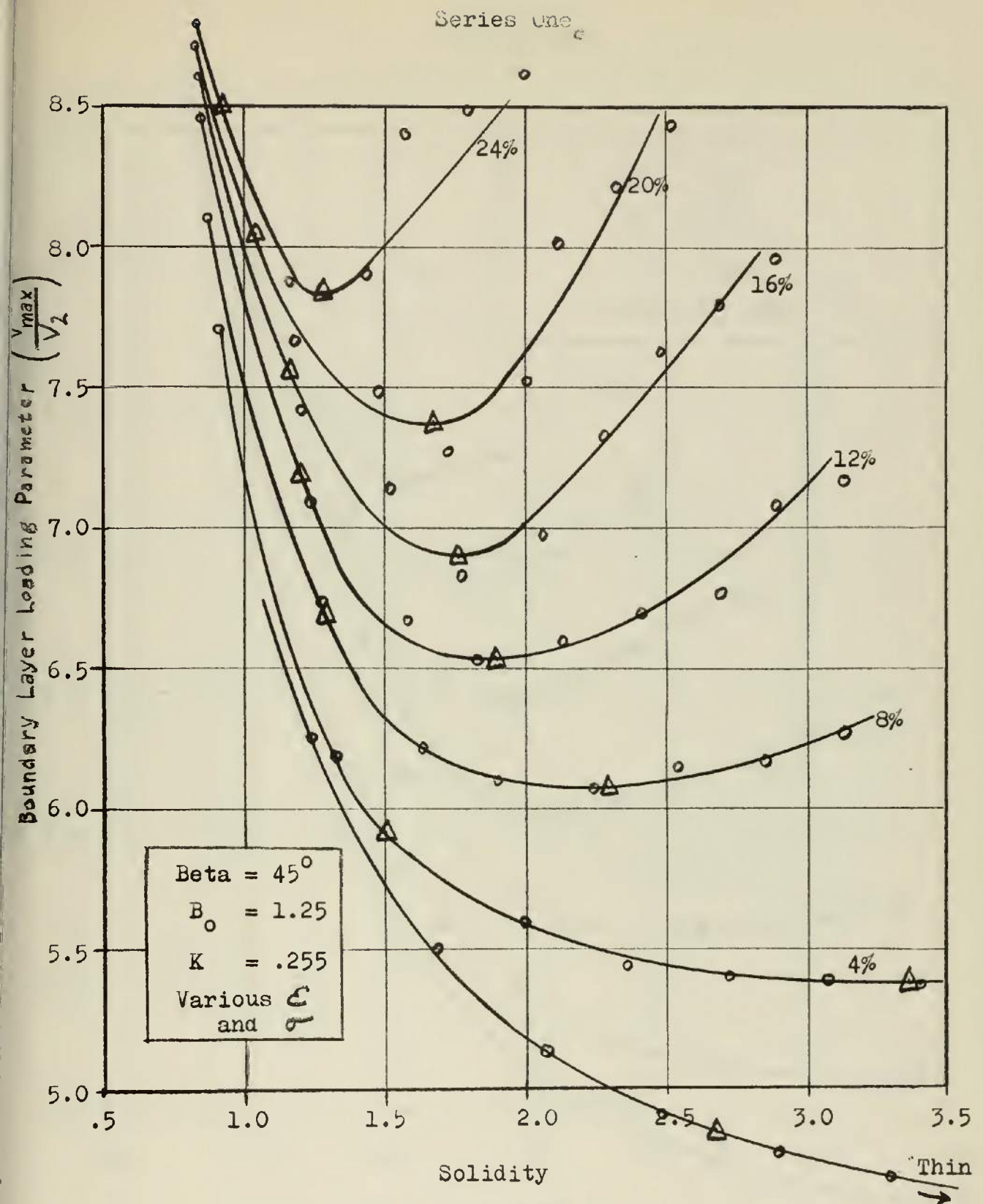
Figure 8.

Boundary Layer Loading Parameter vs. Solidity
For Constant Thickness Airfoils
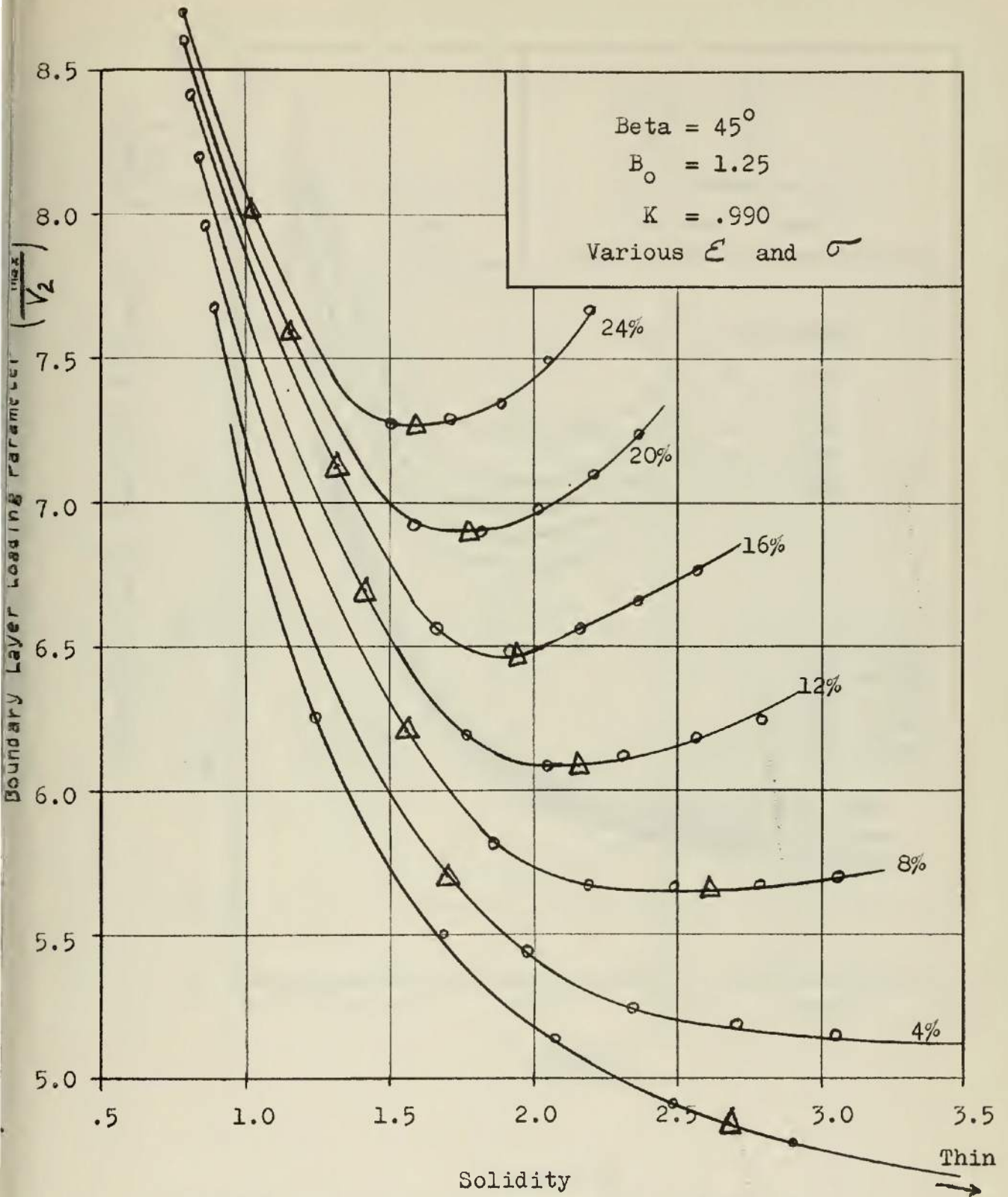
Figure 9.

Boundary Layer Loading Parameter vs. Solidity

For Constant Thickness Airfoils
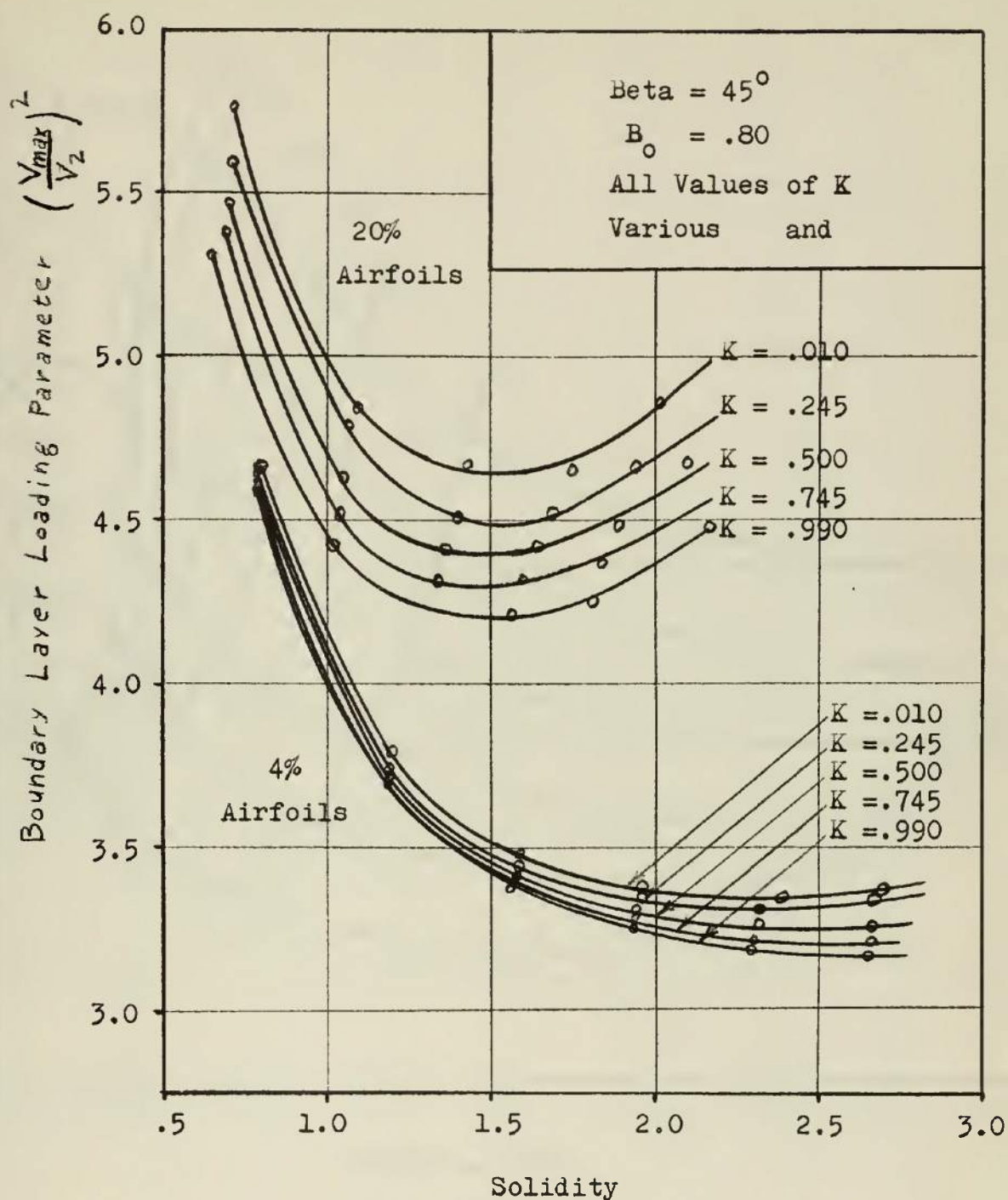
Figure 10.

Boundary Layer Loading Parameter vs. Solidity
Showing the Effect of Parameter K Variations

44
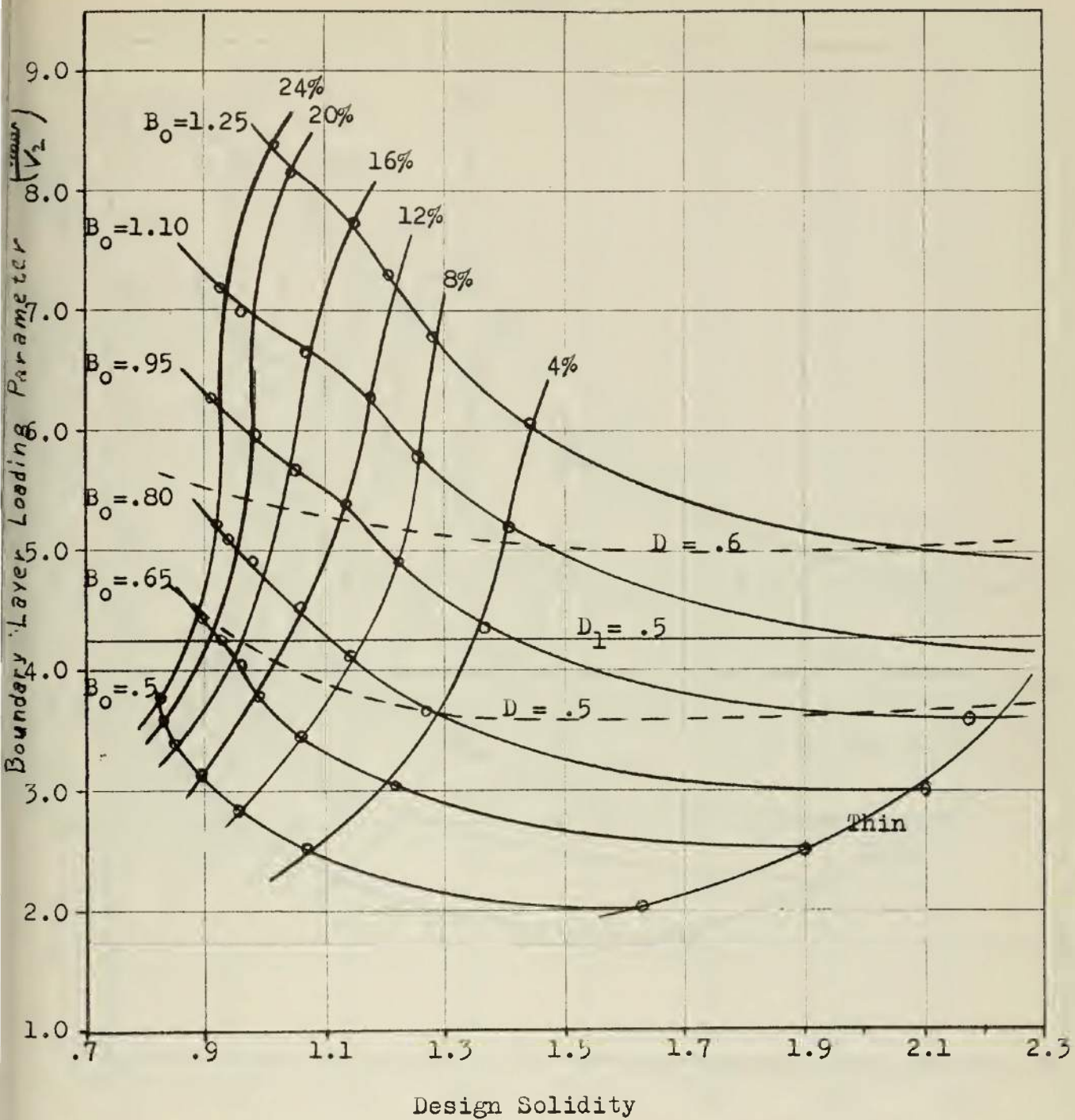
Figure 11.

Boundary Layer Loading Parameter vs. Design Solidity

For Various Cascades   Beta = 45° K = .010

45
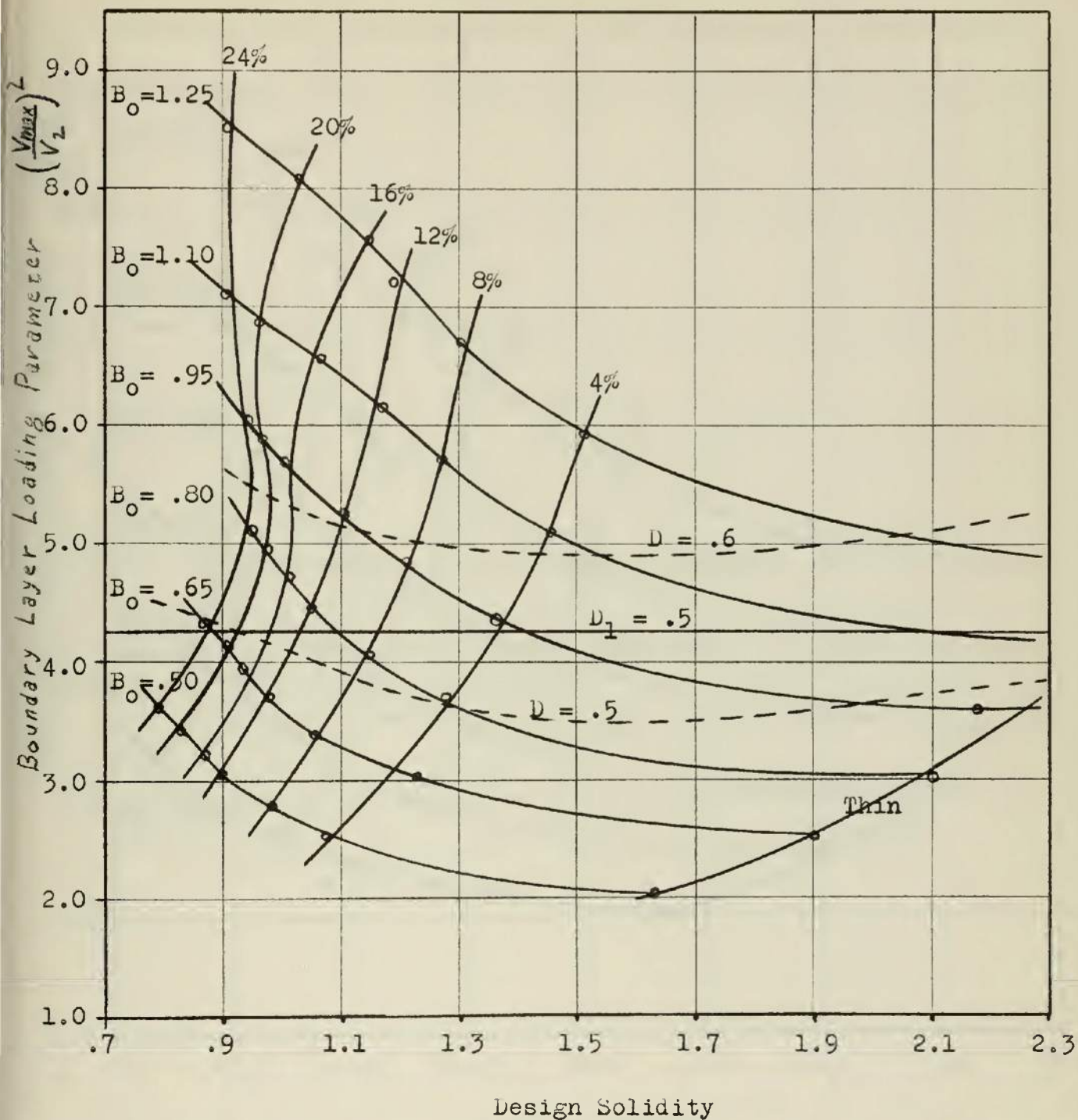
Design Solidity

Figure 12.

Boundary Layer Loading Parameter vs. Design Solidity

For Various Cascades   Beta = 45°   K = .255
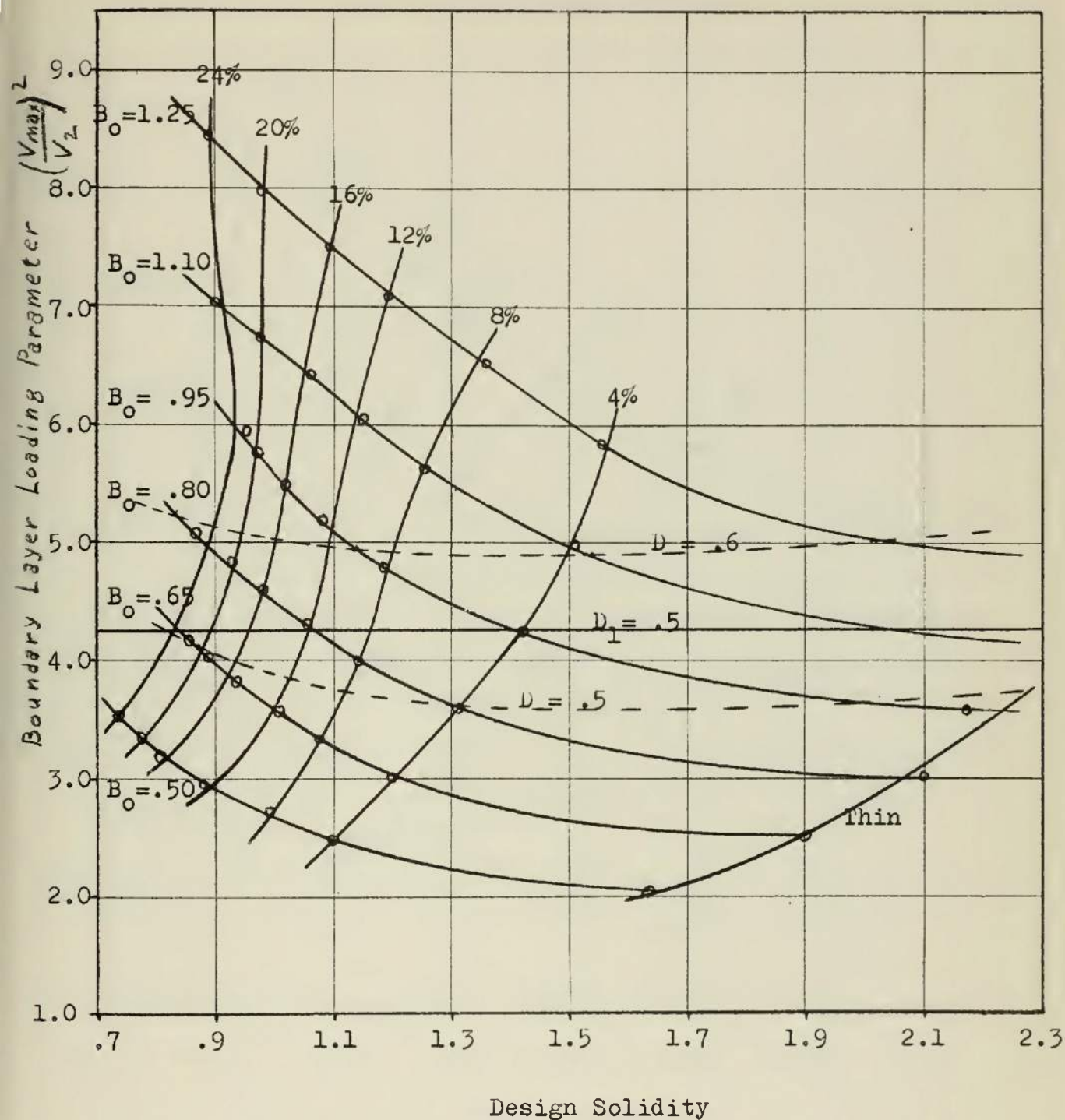
Design Solidity

Figure 13.

Boundary Layer Loading Parameter vs. Design Solidity

For Various Cascades   Beta = 45° K = .500
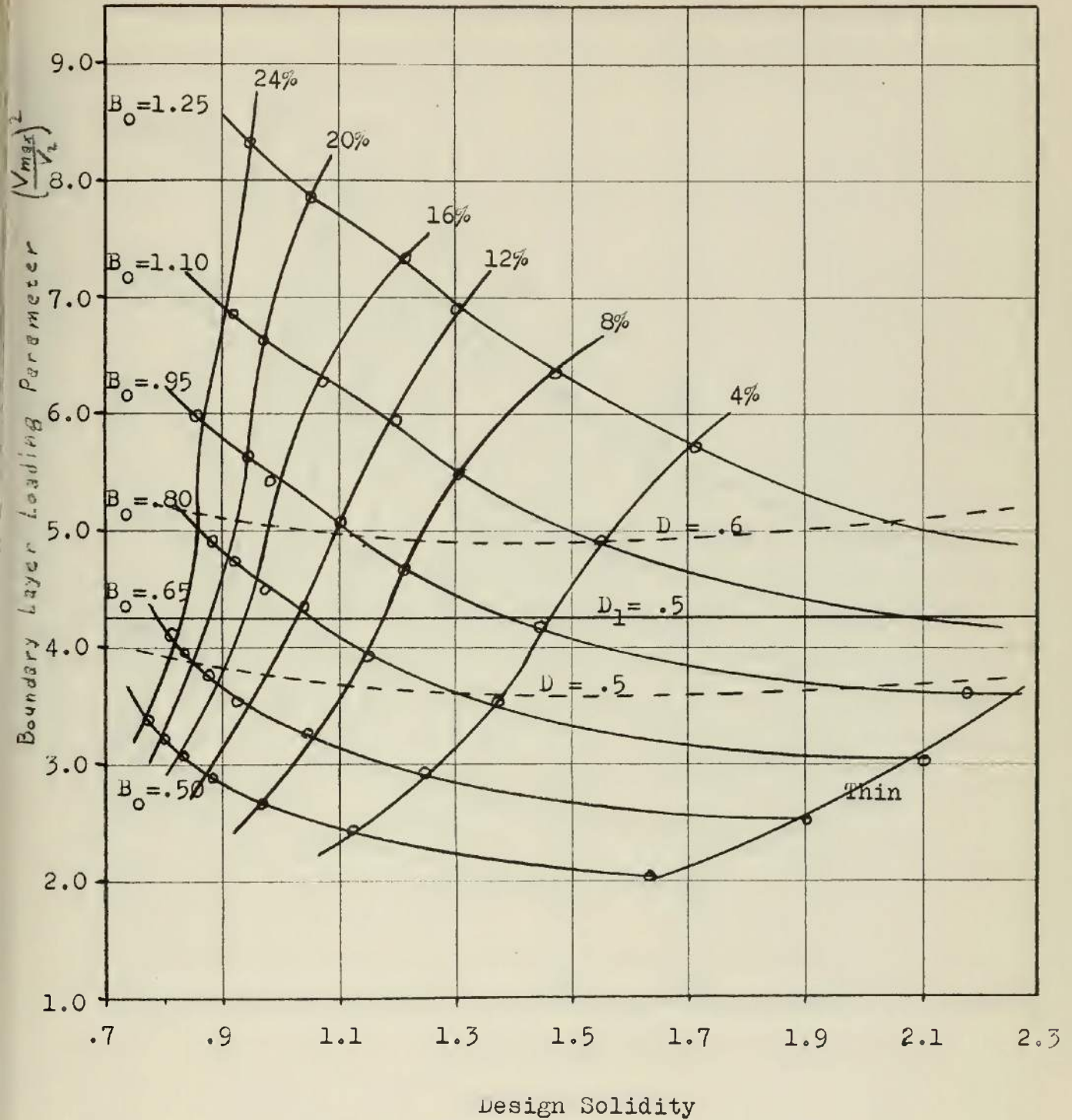
Figure 14.

Boundary Later Loading Parameter vs. Design Solidity
For Various Cascades   Beta = 45°   K = .745

48
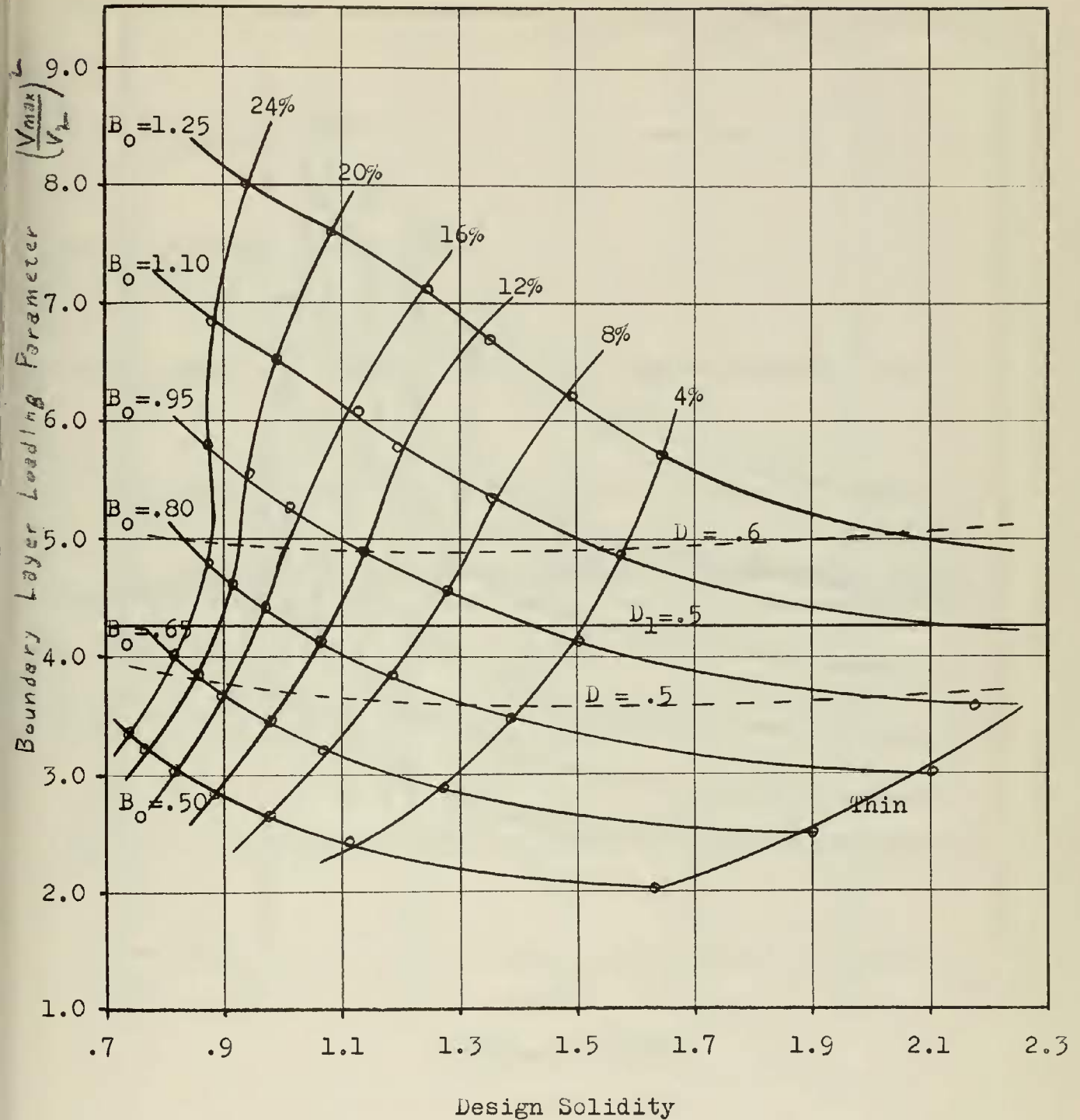
Figure 15.

Boundary Layer Loading Parameter vs. Design Solidity
for Various Cascades   Beta = 45°   K = .990
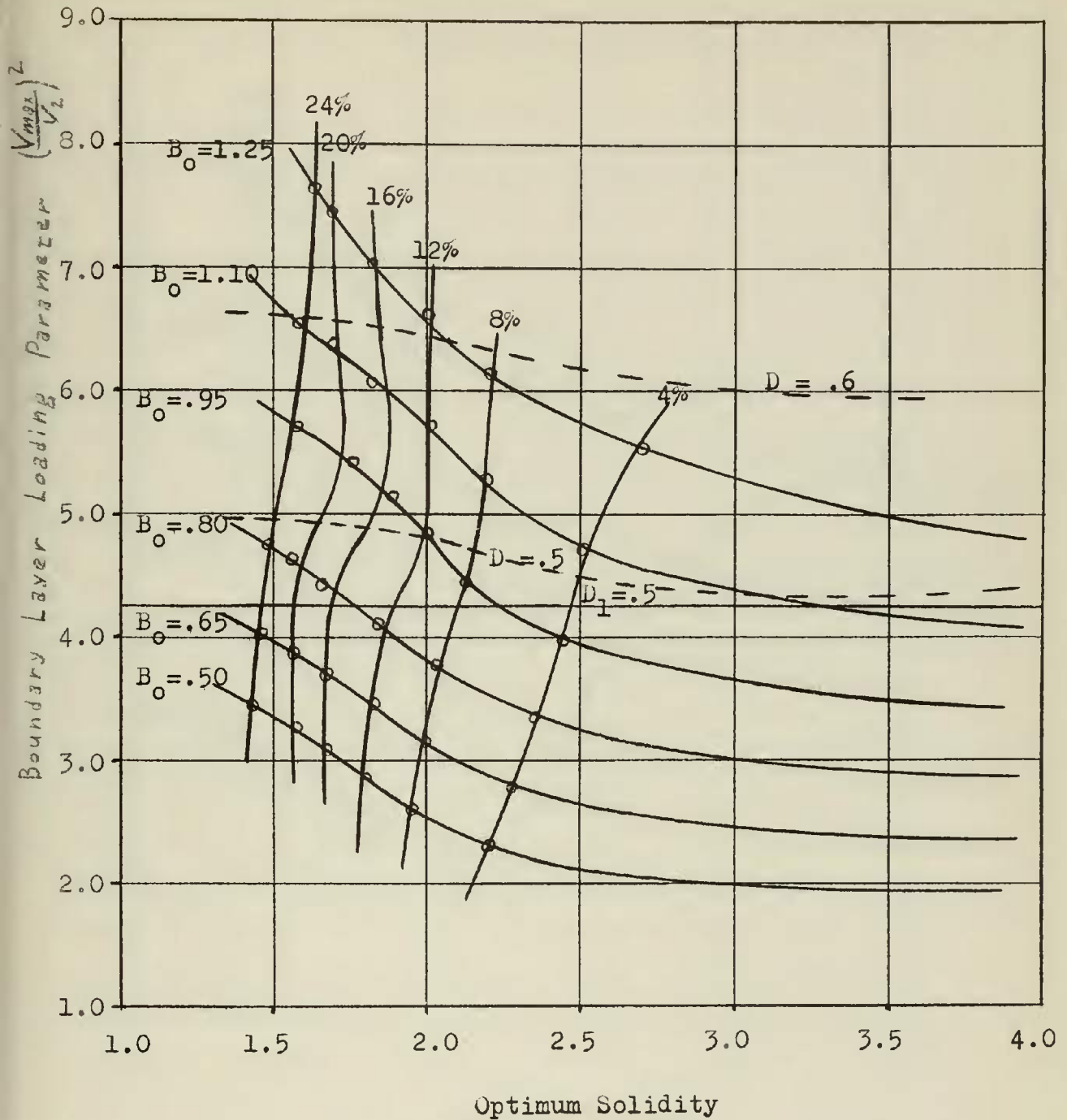
Figure 16.

Boundary Layer Loading Parameter vs. Optimum Solidity

For Various Cascades   Beta = 45°   K = .010
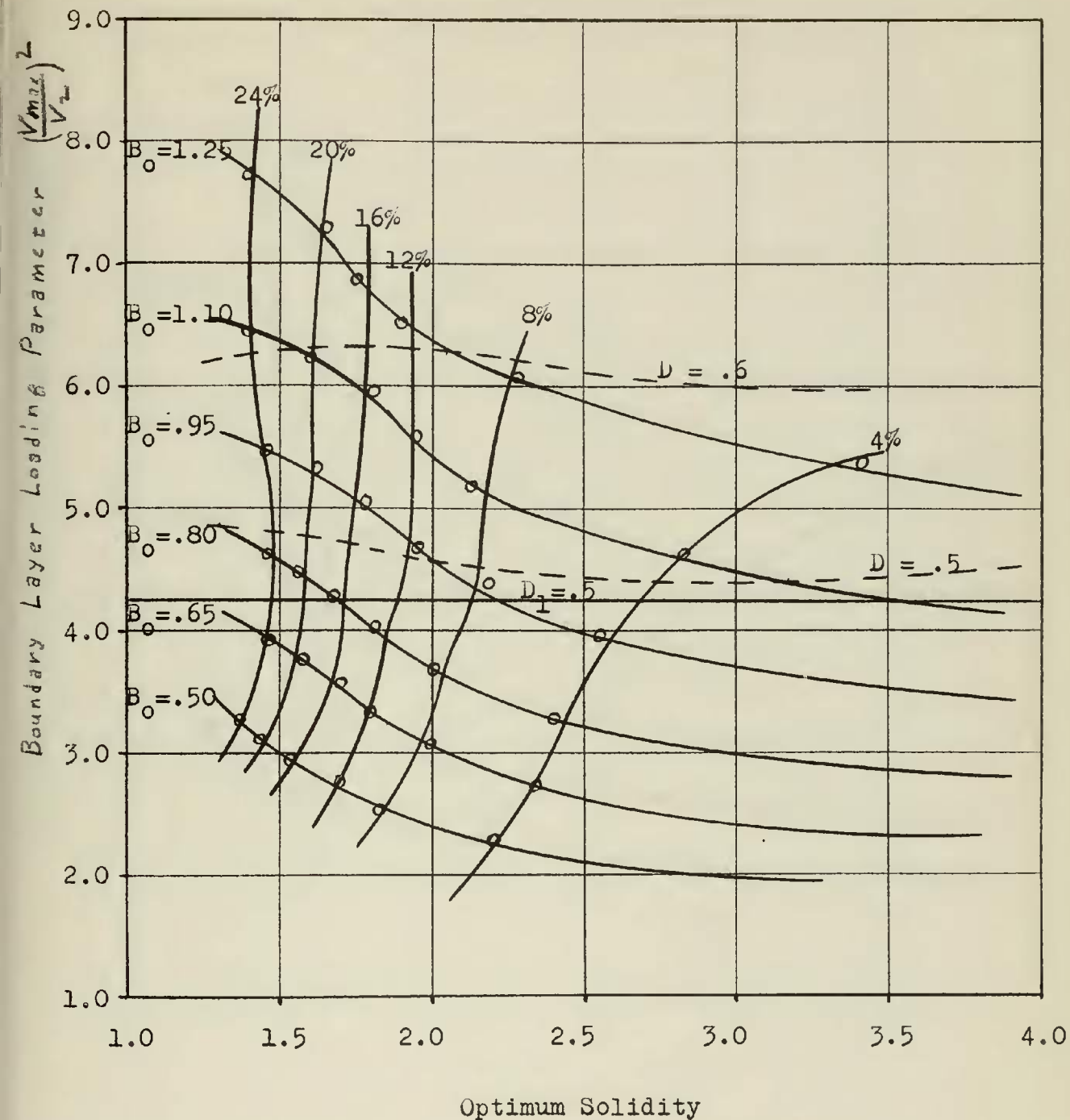
Figure 17.

Boundary Layer Loading Parameter vs. Optimum Solidity

For Various Cascades   Beta = 45° K = .245
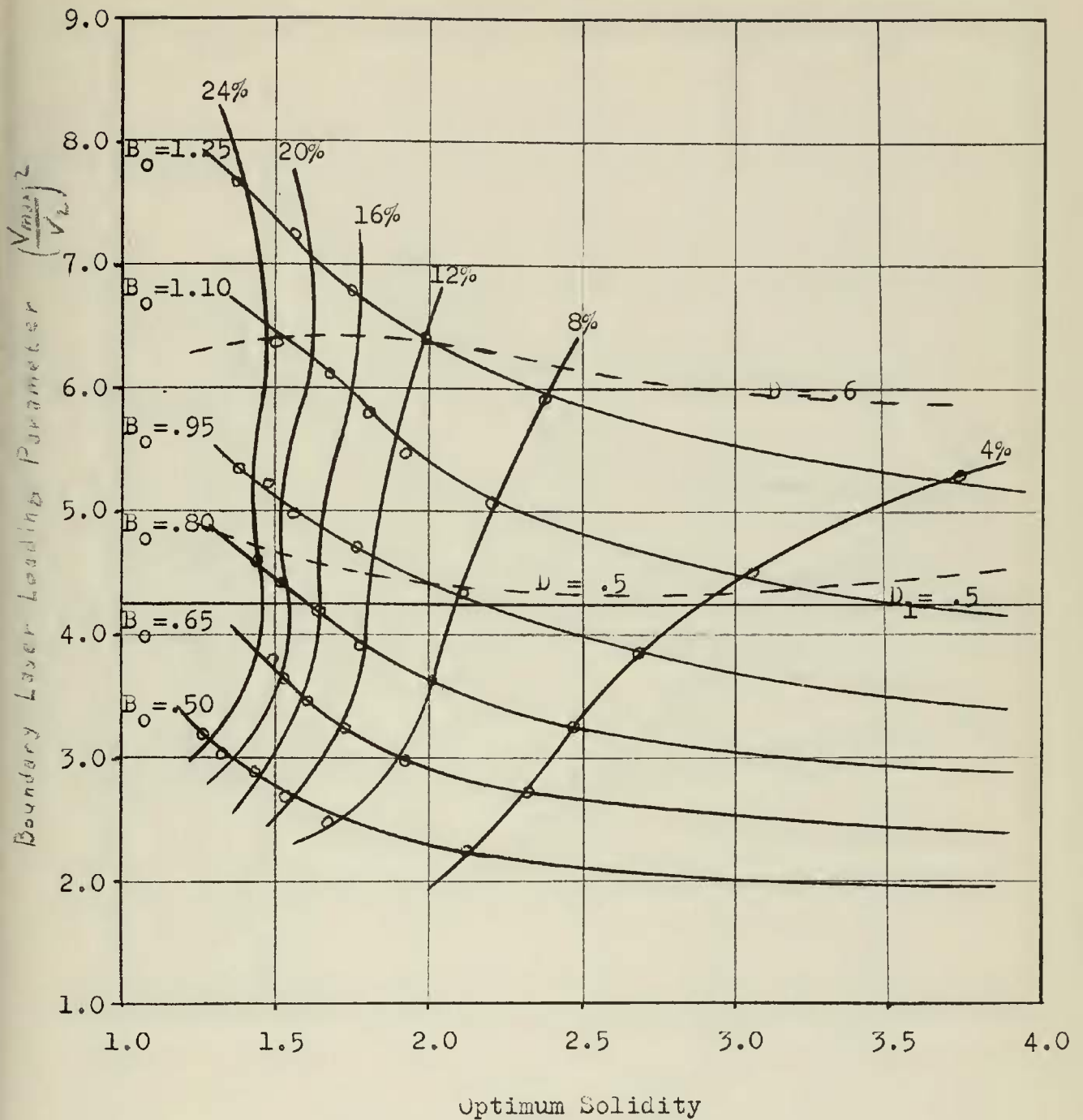
Figure 18.

Boundary Layer Loading Parameter vs. Optimum Solidity
For Various Cascades   Beta = 45°   K = .500
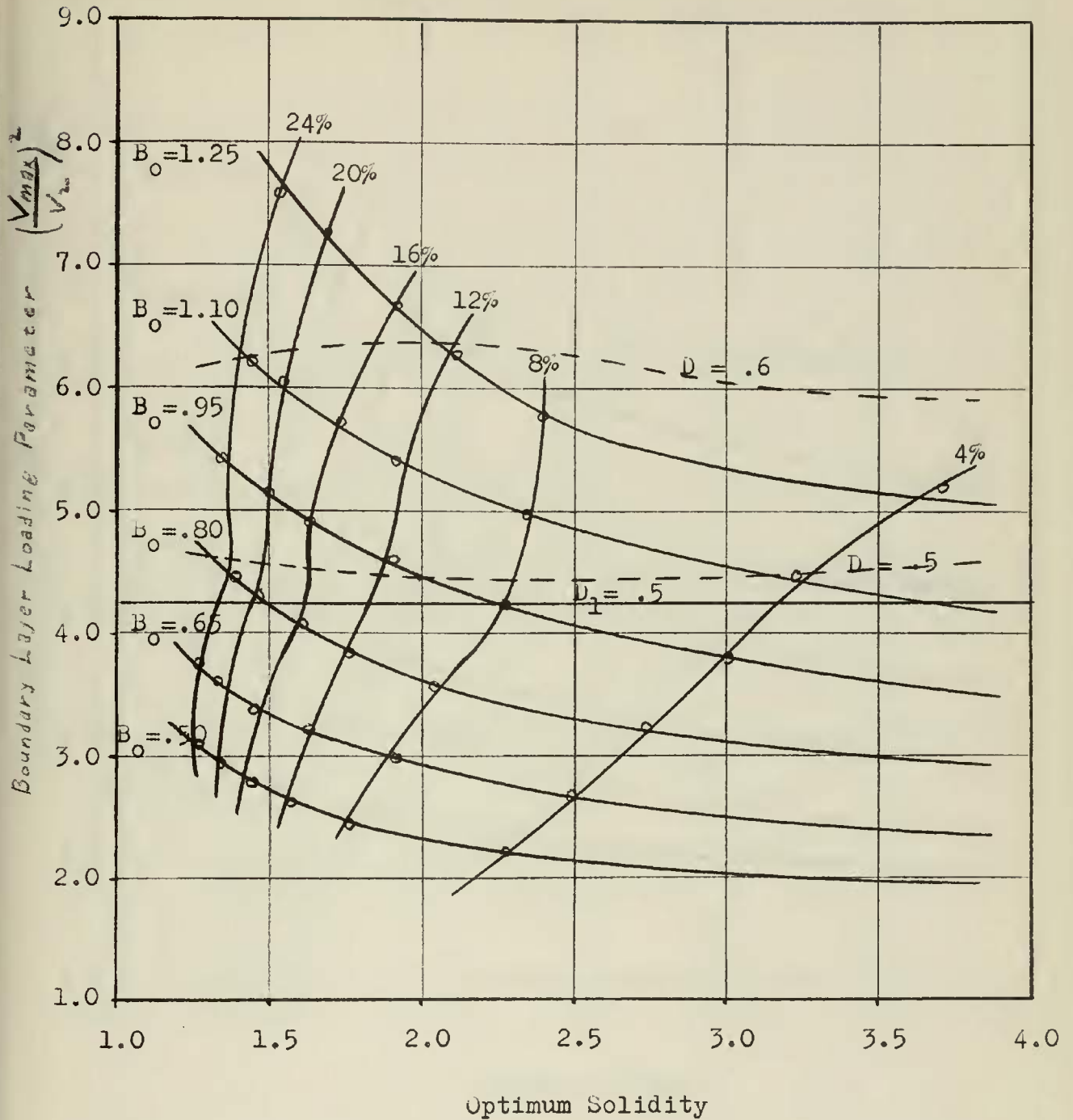
Figure 19.

Boundary Layer Loading Parameter vs. Optimum Solidity
for Various Cascades   Beta = 45° K = .745

53
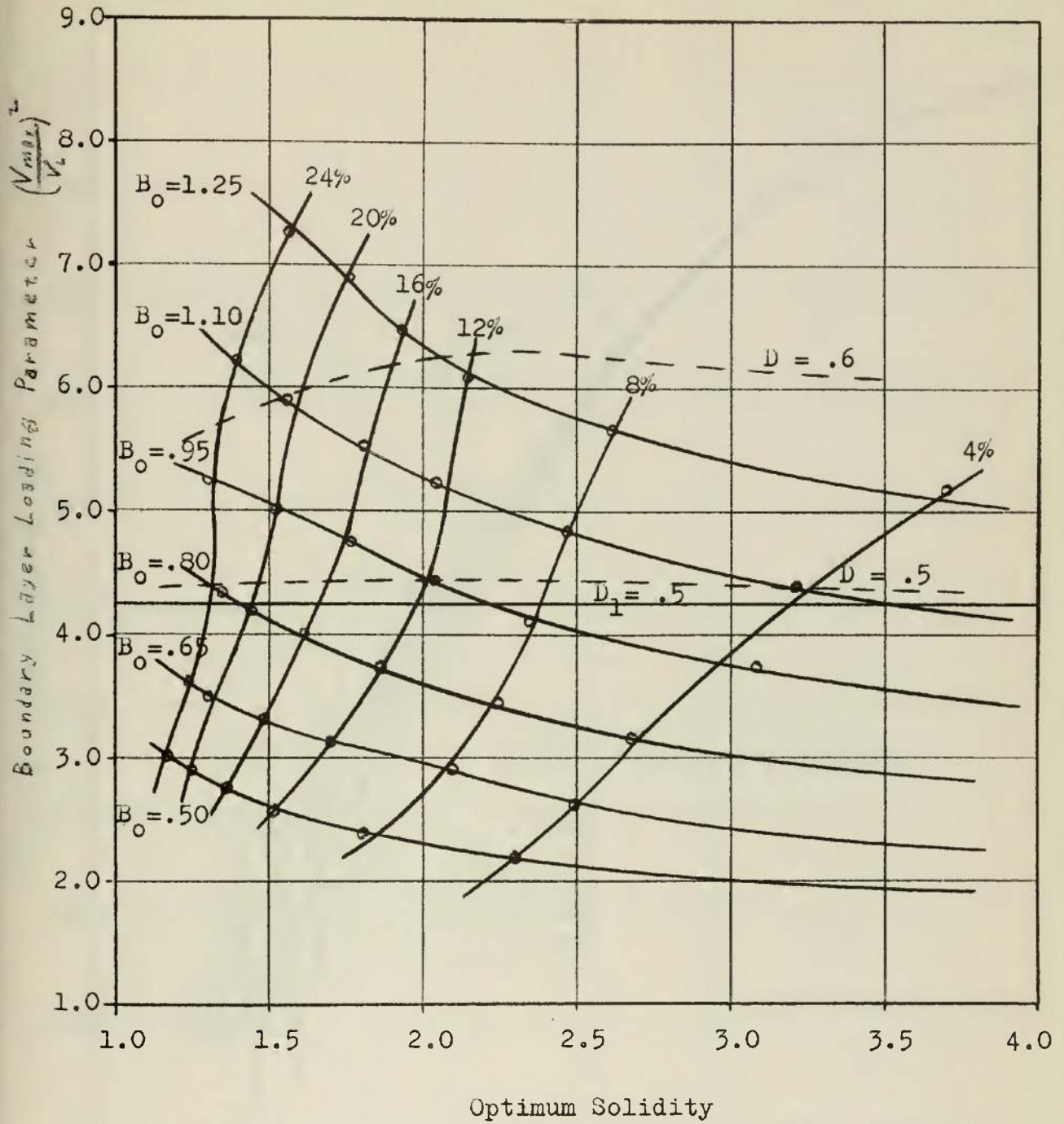
Figure 20.

Boundary Layer Loading Parameter vs. Optimum Solidity
for Various Cascades   Beta = 45°   K = .990
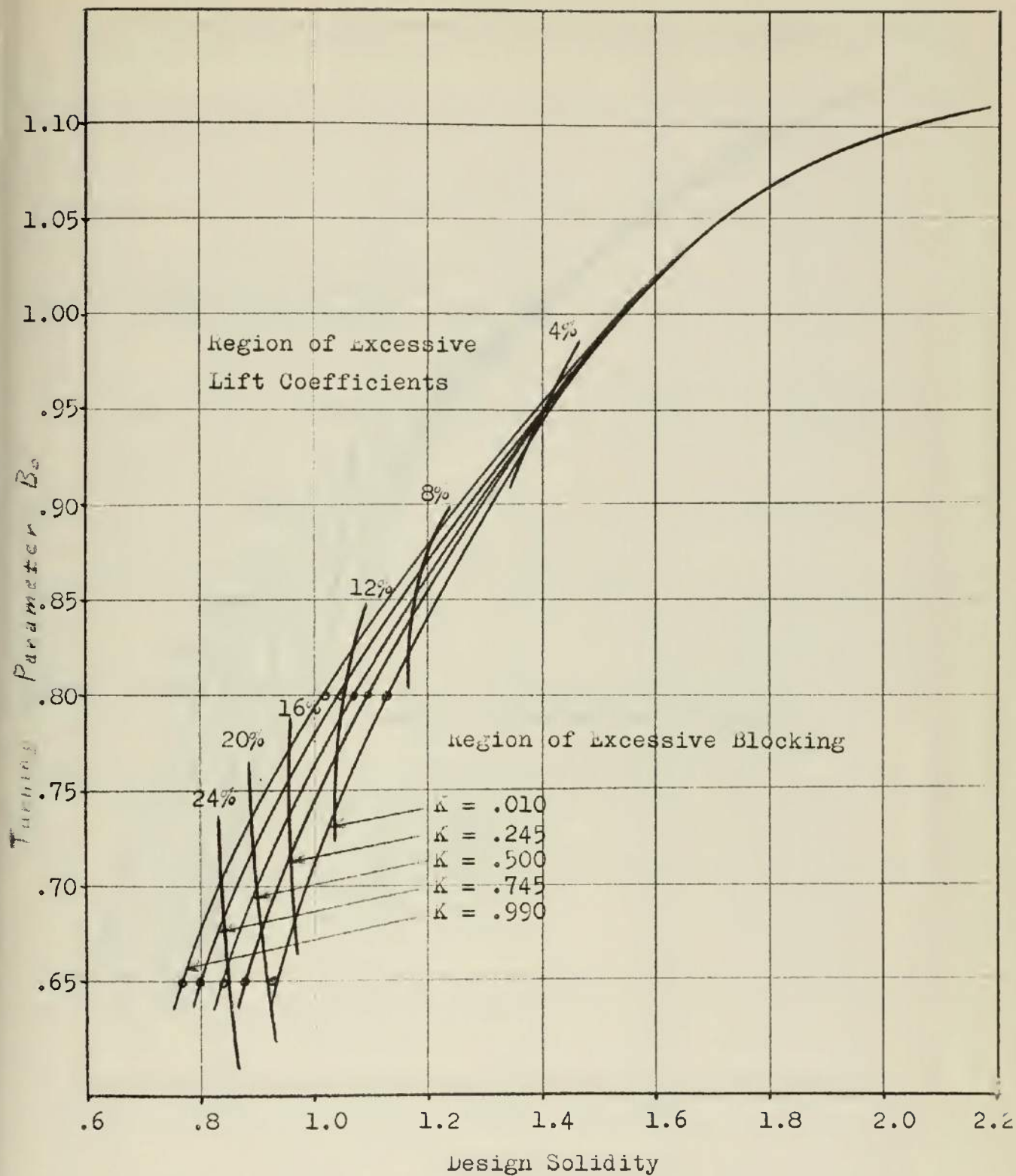
Figure 21.

Turning Parameter vs. Design Solidity

For Boundary Layer Loading Parameter of 4.25

(Corresponds to NASA Local Diffusion Factor of .5)

55
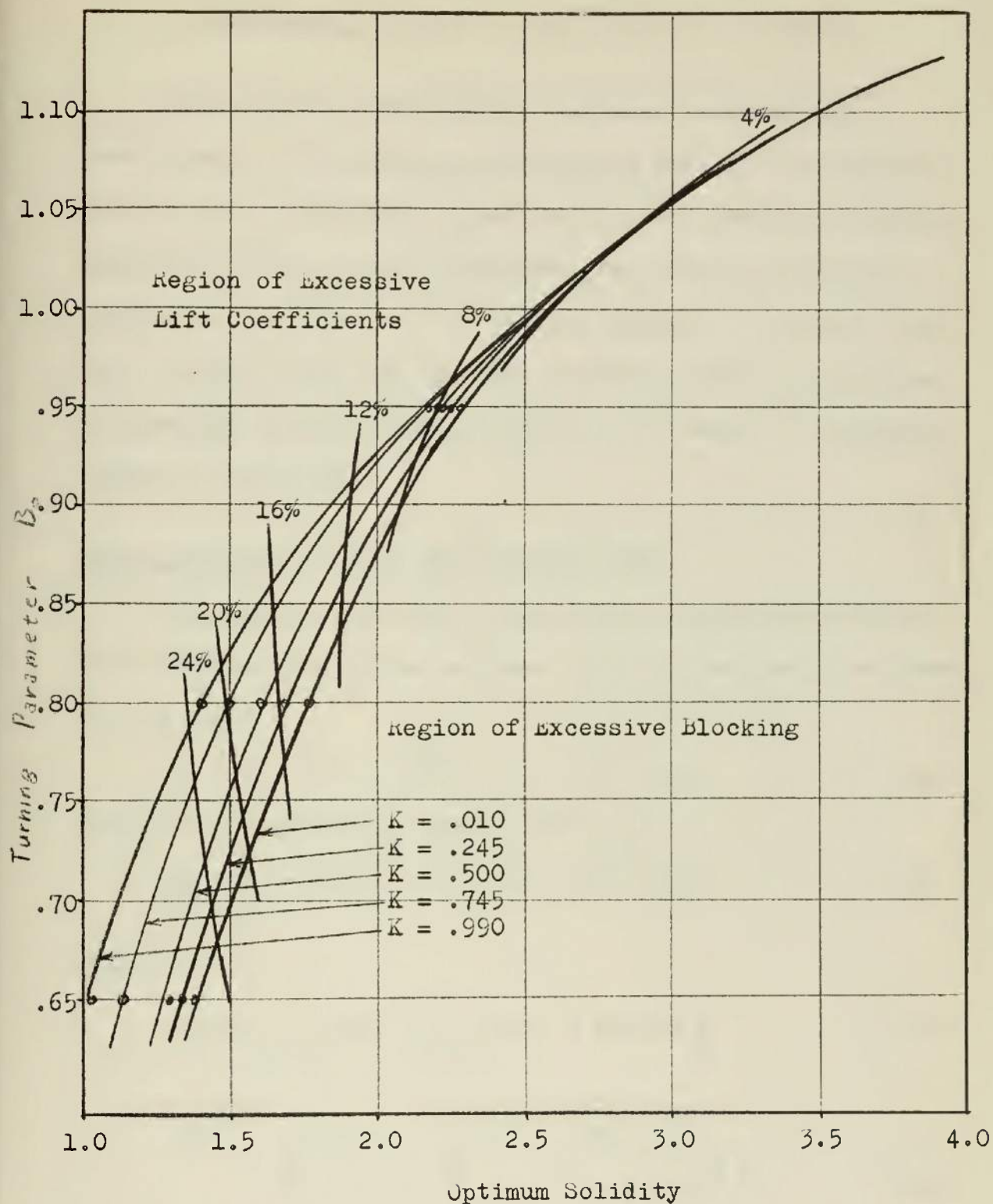
Figure 22.

Turning Parameter vs Optimum Solidity

For Boundary Layer Loading Parameter of 4.25

(Corresponds to NASA Local Diffusion Factor of .5)

56

MATHEMATICAL ANALYSIS OF THE METHOD OF DESIGN

This appendix describes the general mathematical development of the method of designing airfoils in cascade. Some of the fine details, particularly on iterative proceedures, have been omitted. However, the entire calculation proceedure is given in the FORTRAN program in the next appendix. This, along with the explanations given in the table of symbols, should allow analysis of the method to whatever extent is necessary.

Basic Relations in the Near Circle Plane

The complex potential for the flow around the infinite row of closed bodies in the near circle plane may be written in the form:

$$w = \varphi + i\psi = e^{-i\beta}z + (A + iB) F_1(z) \qquad \text{A1a}$$

With the corresponding complex velocity:

$$\frac{dw}{dz} = v_x - iv_y = e^{-i\beta} + (A + iB) F_2(z) \qquad \text{A1b}$$

where

$$F_1(z) = R_1(x,y) + iJ_1(x,y) = \tfrac{1}{2} \coth \frac{z}{2} \qquad \text{A2a}$$

$$F_2(z) = R_2(x,y) + iJ_2(x,y) = \frac{d}{dz} F_1(z)$$

$$= \frac{d}{dz}\left[\tfrac{1}{2} \coth \frac{z}{2} \right] = -\tfrac{1}{4} \operatorname{csch}^2 \frac{z}{2} \qquad \text{A2b}$$

By expanding these functions and separating them into their real and imaginary parts, it is found that:

57

$$R_1(x,y) = \tfrac{1}{2}\left(\frac{\sinh x}{\cosh x - \cos y}\right) \qquad \text{A3a}$$

$$J_1(x,y) = -\tfrac{1}{2}\left(\frac{\sin y}{\cosh x - \cos y}\right) \qquad \text{A3b}$$

$$R_2(x,y) = -\tfrac{1}{2}\frac{(\cosh x \cos y - 1)}{(\cosh x - \cos y)^2} \qquad \text{A3c}$$

$$J_2(x,y) = +\tfrac{1}{2}\frac{(\sinh x \sin y)}{(\cosh x - \cos y)^2} \qquad \text{A3d}$$

The expressions for velocity potential, stream function, and velocity components now reduce to:

$$\phi = x \cos\beta + y \sin\beta + AR_1(x,y) - BJ_1(x,y) \qquad \text{A4a}$$

$$\psi = -x \sin\beta + y \cos\beta + AJ_1(x,y) + BR_1(x,y) \qquad \text{A4b}$$

$$v_x = \cos\beta + AR_2(x,y) - BJ_2(x,y) \qquad \text{A4c}$$

$$v_y = \sin\beta - AJ_2(x,y) - BR_2(x,y) \qquad \text{A4d}$$

These relations represent the flow without circulation about an infinite series of nearly circular bodies spaced at equal intervals $S = 2\pi$ along the y axis. The contour of a typical body is shown in Figure 5.

Location of Stagnation Points

Due to the interference caused by the presence of the infinite stack of bodies, the stagnation points on any body are displaced slightly from the position they would have occupied if the body were isolated in the flow. For this reason, some computation is necessary to locate these points.

58

Designating the front and rear stagnation points by the subscripts A and B respectively, and noting the type of polar symmetry involved, the following facts are observed. At the two stagnation points, both velocity components vanish by definition. Also, by reason of the odd symmetry involved, $x_A = - x_B$, $y_A = - y_B$, and $\psi_A = -\psi_B$. However, since the points A and B lie on the same streamline, $\psi_A = + \psi_B$. The only way in which these two conditions on ψ can be satisfied is if $\psi_A = \pm \psi_B \equiv 0$. Since the stream function vanishes at the stagnation points, it also vanishes at all other points on the body, since they are on the same streamline.

The velocity potential φ on the other hand varies from a maximum negative value at A to a maximum positive value at B. The value φ_B then defines the amplitude of the φ function on the contour of the body. This amplitude may be arbitrarily prescribed, and will then fix the size of the near circle contour in relation to the fixed spacing $\sigma = 2\pi$.

Let $K_1(x_B, y_B) = K_{1B}$ and so forth. Then, at the point B from the foregoing discussion:

$$\varphi_B = x_B \cos\beta + y_B \sin\beta + AK_{1B} - BJ_{1B} = \text{arbitrary value} \quad \text{A5a}$$

$$\psi = -x_B \sin\beta + y_B \cos\beta + AJ_{1B} + BK_{1B} = 0 \quad \text{A5b}$$

$$v_x = \hspace{3cm} \cos\beta + AK_{2B} - BJ_{2B} = 0 \quad \text{A5c}$$

$$v_y = \hspace{3cm} \sin\beta - AJ_{2B} - BK_{2B} = 0 \quad \text{A5d}$$

59

The last two of the above equations may be solved simultaneously for the unknown constants A and B with the results:

$$A = \frac{- R_{2B} \cos \beta + J_{2B} \sin \beta}{R_{2B}^2 + J_{2B}^2} \qquad \text{A6a}$$

$$B = \frac{+ R_{2B} \sin \beta + J_{2B} \cos \beta}{R_{2B}^2 + J_{2B}^2} \qquad \text{A6b}$$

Substituting these results into the expressions for ϕ_β and ψ yields two equations in which the two unknowns are the coordinates x_B and y_B of the aft stagnation point. The equations are trancendental, however, so that an iteration technique is necessary for solution. Care was necessary in this area as all the functions are multi-valued in y, and the result could converge to a point differing by some integral multiple of 2π in the y dimension from the intended point. The general method involves starting with low values of in effect close to the isolated case where the location of the stagnation points is known, and working up to the desired value by modest increments.

Location of Points on the Contour

Once the location of the aft stagnation point has been found, the constants A and B can be evaluated from equations A6a and A6b . The other points on the contour can then be located from equations A5a and A5b by setting $\psi = 0$ and assigning a suitable value to ϕ . This computer program

60

divides the interval from $-\rho_B$ to $+\rho_B$ into 20 equal parts.
This yields 20 points along each surface of the airfoil, or
40 points in all. As pointed out in the text, it would be
helpful to subdivide some of these intervals near the leading
edge to get a better check on the maximum velocity in this
critical region.

The equations for the location of these contour points
are again trancendental, and a similar iterative technique
is necessary for solution. Once the coordinates of a point
are known, the velocity components are found from equations
A5c and A5d. The final velocity v and the slope $\propto$ of the
contour at that point are found from the relations:

$$v = \sqrt{v_x^2 + v_y^2} \qquad\qquad \text{A8a}$$

$$\propto = \arctan \frac{v_y}{v_x} \qquad\qquad \text{A8b}$$

At the stagnation points, this relation becomes indeterminate
and L'Hopital's rule is used for a solution.

Basic Relations in the Circle Plane

It is well known that the flow around an infinite row
of arbitrary but identical contours can in principle be
mapped into a corresponding flow about a single unit circle.
If the flow is of zero circulation, and the direction of flow
far from the contours is β then the corresponding flow in
the circle plane is expressed by the following complex po-
tential and velocity:

$$w = \phi + i\psi = e^{-i\beta} \ln\left(\frac{\zeta + e^{\gamma}}{\zeta - e^{\gamma}}\right) + e^{+i\beta} \ln\left(\frac{\zeta + e^{-\gamma}}{\zeta - e^{-\gamma}}\right) \qquad \text{A9a}$$

$$\frac{dw}{d\zeta} = (v_h - iv_\theta)\, e^{-i\theta} = e^{-i\beta}\left(\frac{-2e}{\zeta - e^{2\gamma}}\right) + e^{+i\beta}\left(\frac{-2e^-}{\zeta^2 - e^{-2\gamma}}\right) \qquad \text{A9b}$$

Splitting these into real and imaginary parts, and placing r =a = 1 leads to the result that along the unit circle,

$$V_R = 0 \qquad\qquad \text{A10a}$$

$$\psi = \text{constant} \qquad\qquad \text{A10b}$$

This verifies that the circle is in fact a streamline. Further, along this circle:

$$\phi = \cos\beta \ln\left(\frac{\cosh\gamma + \cos\theta}{\cosh\gamma - \cos\theta}\right) + \sin\beta \cdot 2 \arctan\left(\frac{\sin\theta}{\sinh\gamma}\right) \qquad \text{A11a}$$

$$V_\theta = 4\left[\frac{\cos\beta \cosh\gamma \,\sin\theta + \sin\beta \sinh\gamma \,\cos\theta}{\cosh 2\gamma - \cos 2\theta}\right. \qquad \text{A11b}$$

Singularities and stagnation points in the Circle Plane

To find the stagnation point B, set $V_\theta = 0$. Then equation A11b gives:

$$\tan\theta_B = \tan\beta \,\tanh\gamma \qquad\qquad \text{A12}$$

Substituting this into equation A11A produces a result which can be reduced to the form:

62

$$\phi_B = \cos\beta \ \ln\left(\frac{T + \cos\beta}{T - \cos\beta}\right) + \sin\beta \cdot 2 \arctan\left(\frac{\sin\beta}{T}\right) \qquad A13a$$

where

$$T = \sqrt{\tfrac{1}{2}(\cosh 2\gamma + \cos 2\beta)} \qquad A13b$$

These equations then must be solved for T then γ for assigned values of β and ϕ_B which must be the same as the values for β and ϕ_B previously employed in the near circle plane. Since the functions are trancendental, an iterative technique is again required. Newton's method is employed, which involves calculation of the derivative $\dfrac{\partial \phi_B}{\partial T}$. Denoting this by the symbol ϕ_B' then:

$$\phi_B' = \frac{-8T^2}{\left(2T^2 - \cos 2\beta\right)^2 - 1} \qquad A14$$

Applying the equations in this form however, requires an excessive number of significant figures in the evaluation of T. To circumvent this problem, the following sublitution was used to eliminate T.

$$T = \cos\beta + \Delta T \qquad A15$$

The previous equation then become

$$\phi_B = \cos\beta \ \ln\left[\frac{2\cos\beta + \Delta T}{\Delta T}\right] + \sin\beta \cdot 2 \arctan\left[\frac{\sin\beta}{\cos\beta + \Delta T}\right]$$

$$A16a$$

63

$$\varphi'_B = -\left(\frac{2}{\Delta T}\right)\left(\frac{\cos\beta + \Delta T}{2\cos\beta + \Delta T}\right) \frac{(\cos\beta + \Delta T)}{\left[1 + (2\cos\beta + \Delta T)\Delta T\right]} \qquad \text{A16b}$$

The problem of finding T for assigned values of β and φ_B by Newton's method has no difficulty with regard to significant figures. The parameter γ and its hyperbolic functions may now be found from:

$$\sinh\gamma = \sqrt{T(2\cos\beta + \Delta T)} = \sqrt{\tfrac{1}{2}(\cosh 2\gamma - 1)} \qquad \text{A17}$$

The initial estimate for Newton's method is obtained by neglecting T in the last term of equation A16a . The resulting equation may be solved explicitly for ΔT .

$$\Delta T = \frac{2\cos\beta}{\left(e^P - 1\right)} \qquad \text{A18a}$$

where

$$P = \left(\frac{\varphi_B - 2\beta\sin\beta}{\cos\beta}\right) \qquad \text{A18b}$$

These expressions provide an excellent first estimate for T, and in fact for the special case of $\beta = 0$, they are exact.

With β and γ known, the location of any point Θ_i having an assigned value of φ_i is defined implicitly by equation A11a. To establish the location of points corresponding to those in the near circle plane, all that is necessary is to have the respective values of φ_i be the same in

64

the two planes. As before, an iterative solution is required.

Circulation

The complex potential and velocity for a purely circulatory flow of unit circulation in the circle plane are as follows:

$$\Delta w = - \frac{i \cos \beta}{2} \ln \left(\frac{\varsigma^2 - e^{+2\gamma}}{\varsigma^2 - e^{-2\gamma}} \right) \qquad \text{A19a}$$

$$\frac{d(\Delta w)}{d\varsigma} = \frac{-2i \cos \beta \sinh \gamma \varsigma}{\varsigma^4 - 2 \cosh \beta \cdot \varsigma^2 + 1} \qquad \text{A19b}$$

$$\varsigma = r e^{i\theta} \qquad \text{A19c}$$

Separating these into real and imaginary parts, it is again found that the unit circle $r = 1$ is a streamline, along which the velocity distribution is given by

$$\Delta V_\theta = \frac{- \sinh 2\gamma}{\cosh 2\gamma - \cos 2\theta} \qquad \text{A20}$$

This circulatory component must be evaluated at the same points θ_i previously established around the periphery of the circle. By superposition, the total velocity at these points is then given by:

$$\mathcal{U}_\theta = V_\theta + \Box_0 \Delta V_\theta$$

65

Stagnation Points with circulation in Circle Plane

Just as the stagnation points A and B are defined by the condition $V = 0$, so are the stagnation points L and T defined by the corresponding condition $\mathcal{U}_\theta = 0$. Introducing this condition into the foregoing equations yields the essential result

$$\Theta_B - \Theta_T = \Theta_L - \Theta_A = \gamma = \arcsin\left[\frac{B_o}{4} \cdot \frac{\sinh 2\gamma \cos \Theta_c}{\cosh \gamma \cos \beta}\right.$$

A22

Once the points L and T have been located in the circle plane, the corresponding values of $\mathcal{P}_L$ and $\mathcal{P}_T$ may be found from equation A11a. Introducing these values into the near circle plane leads to the location of the points L and T in that plane by solving equations A4a and A4b.

Mapping Detween Circle and Near Circle Planes

Mapping between the circle cr ζ plane and the near circle or z plane, as implied in the preceeding discussion, is accomplished despite the fact that no explicit function for z in terms of ζ or vice-versa is known. The mapping is done implicitly through the fact that the non-circulatory flows in the two planes must correspond. Or in other words, through the condition that

$$w(z) = w(\zeta)$$

A23a

Differentiating this gives

$$\left|\frac{dw}{dz}\right| = \frac{\left|\frac{dw}{d\zeta}\right|}{\left|\frac{dz}{d\zeta}\right|}$$ A23b

But

$$\left|\frac{dw}{dz}\right| = v$$ A23c

and

$$\left|\frac{dw}{d\zeta}\right| = V_\Theta$$ A23d

Hence the mapping derivative becomes

$$\left|\frac{dz}{d\zeta}\right| = \frac{V_\Theta}{v}$$ A23e

The flow with circulation has been completely defined in the foregoing development for the circle plane. In the near circle plane, however, only the non-circulatory flow has been explicitly defined. As explained in the text, adding circulation terms to the complex potential in the near circle plane produces unwanted distortions. Therefore, the method used is to map the known flow with circulation in the circle plane back into the near circle plane using the mapping relations previously established. These mapping relations are of course independent of circulation. Thus, for the final flow with circulation

$$w_c (z) = w_c (\zeta) = w (\zeta) + B_0 \Delta w (\zeta)$$ A24a

Differentiating this gives

$$\left|\frac{dw_c}{dz}\right| = \frac{\left|\frac{dw}{d\zeta} + B_0 \frac{d(\Delta w)}{d\zeta}\right|}{\left|\frac{dz}{d\zeta}\right|} \qquad \text{A24b}$$

Substituting in terms of velocities, and introducing proper algebraic signs gives finally for the velocity in the near circle plane:

$$\mathcal{V} = \frac{V_\Theta + B_0 \Delta V_\Theta}{\dfrac{V_\Theta}{v}} = v + B_0 \Delta V_\Theta\left(\frac{v}{V_\Theta}\right) \qquad \text{A25}$$

Basic Relations in the Cascade Plane

The basic idea of this entire method is to map the near circles into a cascade of airfoils in much the same manner that the Joukowski transformation may be used to map a single circle into an airfoil. The equations for the transformation are identical in form to those already developed for the flow in the near circle plane. However, all coordinates are evaluated with respect to axes shifted slightly from the original position. Denoting these shifted coordinates by primes, the mapping function employed is specifically:

$$\zeta^* = \xi + i\eta = e^{-i\beta'}z' + (A' + iB')\, F_1(z') \qquad \text{A25a}$$

$$\frac{d\zeta^*}{dz'} = u_x - iu_y = e^{-i\beta'} + (A' + iB')\, F_2(z') \qquad \text{A25b}$$

Where

$$F_1(z') = \tfrac{1}{2} \coth \frac{z'}{2} \qquad\qquad\qquad \text{A26a}$$

$$F_2(z') = -\tfrac{1}{4} \operatorname{csch}^2 \frac{z'}{2} \qquad\qquad \text{A26b}$$

Note that the above functions are exactly of the same form as equations A1 and A2 . All subsequent results may readily be obtained through this analogy.

Determination of Airfoil Shape

In order to transform the near circle into the required airfoil shape, it is necessary to locate the singular points P and Q of the mapping transformation in the proper relation to the stagnation points L and T of the flow. Normally, P is located a short distance inside the contour, just opposite L on the surface. Similarly, point Q lies inside the contour on a line normal to the contour at T. Refer to Figure 5. The significance of these locations may be qualitatively understood from the fact that as the relative distance $\frac{PL}{R_B}$ $= \mathcal{E}$ is made small, the radius of curvature at the nose of the airfoil decreases rapidly, and in the limit, as $\mathcal{E} = 0$ the nose becomes cusped. Similarly, the relative distance $\frac{QT}{R_B} = \mathcal{E}K$ controls the tail curvature. In the limit as $\mathcal{E}K = 0$ the tail becomes cusped in the manner of a Joukowski airfoil. The origin of coordinates for the transformation is shifted from the original location, the midpoint

69

between points A and B , to the new location, the midpoint between points P and Q.

Velocity and Slope Along the Airfoil

The complex potential including circulation in the cascade and near circle planes may be equated

$$w_c\ (\zeta*) = w_c(z) \qquad \text{A27a}$$

Differentiating

$$\frac{dw_c}{d\zeta*} = \frac{\dfrac{dw_c}{dz}}{\left(\dfrac{d\zeta*}{dz'}\right)\left(\dfrac{dz'}{dz}\right)} \qquad \text{A27b}$$

Let

$$\left(\frac{dw_c}{d\zeta*}\right) = Ve^{-i\delta} \qquad \begin{array}{l}\text{conjugate of velocity}\\ \qquad\text{on airfoil}\end{array} \qquad \text{A27c}$$

$$\left(\frac{dw_c}{dz}\right) = \mathcal{U}e^{-i\alpha} \qquad \text{A27d}$$
$$\begin{array}{l}\text{conjugate of velocity}\\ \text{on near circle}\end{array}$$

$$\left(\frac{d\zeta*}{dz'}\right) = ue^{-i\alpha'} \qquad \text{A27e}$$

$$\left(\frac{dz'}{dz}\right) = 1 \qquad \text{A27f}$$

From which, after separating amplitudes and phase angles:

$$V = \frac{\mathcal{U}}{u} = \frac{v + B_0 \Delta V_\theta\left(\dfrac{v}{V_\theta}\right)}{u} \qquad \text{A28a}$$

$$\delta = \alpha \cdot \alpha' \qquad \text{A28b}$$

Fortran Program "Cascade" and Operating Instructions

On the following pages is the FORTRAN program "Cascade"
used in deriving the data used in this study. Input data is
by means of data cards inserted at the end of the program.
Any number of data cards may be used. The first card indica-
tes how many additional data cards are to be read.

Each additional card lists the number of values of the
parameters , , B_o , and K to be computed, their
initial values, and the increment by which each value increa-
ses. Also listed are the print control quantities NOPR and
NEXPR, which control the extent of the print out as indica-
ted in the table of symbols. The computer then calculates
results for every possible combination of the five parameters,
prints the results, and then proceeds to the next card.
The standard print out contains the five input parameters,
the solidity and stagger angle of the cascade, the airfoil
thickness, and the coordinates, slope, velocity, and boundary
layer parameter for each of the 42 points of the airfoil.

Condensed Print Out

when surveying large numbers of cascades, as was done
for this study, it is convenient to condense the data to
reduce the volume of output. Page 83 shows the modifications
made to the basic program to accomplish this. Briefly, all

of the standard print commands were removed. Then commands
to print the heading only were inserted early in the program
right after changes in sigma. The modified print out then
contains no airfoil data at all except for the maximum value
of the boundary layer parameter. Operation of the program
is identical with the basic program.

Iterative Scheme for Constant Thickness Airfoils

Page 84 shows further modifications made to the basic
program to produce cascades with the desired airfoil thick-
ness. In effect this eliminates the parameter $\mathcal{E}$ since it
is varied as necessary to produce the required thicknesses.
The initial value of $\mathcal{E}$ is still read from the data card, but
the column which indicates the number of $\mathcal{E}$ to be calculated
no longer has significance. The program as written will
demand thicknesses from 4% to 24% in 4% increments. Other
values for thickness can be obtained by modifying the appro-
priate commands. No means of doing this by data cards is
provided. The print out is of the condensed form described
previously.

```
..JOB JENISTA
      PROGRAM CASCADE
      DIMENSION XI(42),YI(42),RI(42),VI(42),ALI(42),AHI(42),DELI(42),TEI
     1(42),     DVI(42),XII(42),ETI(42),  EPI(42), VVI(42),VTI(42) ,YNI(4
     22),XNI( 42), V2I(42)          ,DDI(12),ITITLE (10)
      ID=0
  201 READ 204,IB
  204 FORMAT (1I2)
  202 READ 205,NBE,NSG,NBZ,NEP,NAK,BE1,SG1,BZ1,EP1,AK1,BEI,SGI,BZI,EBI,
     1AKI, NOPR, NEXPR
  205 FORMAT (5I2, 10F5.2,2I2)
C  PART IA CONSTANTS FOR NEAR CIRCLE
      BEJ=BE1
      DO2 J=1,NBE
      BE= (3.141593/180.) * BEJ
      SNBE=SINF(BE)
      CNBE=COSF(BE)
      SGK=SG1
      DO3 K=1,NSG
      PHEB=SGK*3.141593
      C22=SNBE
      C23=CNBE
      IF(K-1) 401,401,402
  401 DRUP=1.5708
      DALP=0.
      SIP=0.
      RUP=0.
      ALP=BE
  402 IF(SGK-SIP-.5) 404,404,403
  403 SIG=SIP+.5
      RU=RUP+DRUP*.5
      ALU=ALP+DALP*.5
      IF(NEXPR) 520,520,518
  518 WRITE OUTPUT TAPE 2,519,DRUP,DALP,SIP,SIG,RUP,RU,ALP,ALU
  519 FORMAT(/  7H DRUP =F8.4,   5X 6HDALP = F9.4, /  6H SIP =F 9.4, 5X
     1   5HSIG =F10.4, 5X 5HRUP =F10.4, 5X 4HRU =F11.4,   5X 5HALP =F10.4,
     2  5X 5HALU =F10.4/  )
  520 CALL BAKER (SIG,XU,YU,RU,ALU,AU,BU,R1U,AJ1U,R2U,AJ2U,.000001,
     1   A2U,ITU,C22,C23,NEXPR)
      DRUP=(RU-RUP)/.5
      DALP=(ALU-ALP)/.5
      SIP=SIG
      RUP=RU
      ALP=ALU
      IF(NEXPR) 522,522,521
  521 WRITE OUTPUT TAPE 2,519,DRUP,DALP,SIP,SIG,RUP,RU,ALP,ALU
  522 CONTINUE
      GO TO 402
  404 RB=RUP+DRUP*(SGK-SIP)
      ALB=ALP+DALP*(SGK-SIP)
      IF(NEXPR) 525,525,523
  523 WRITE OUTPUT TAPE 2,524,DRUP,DALP,SIP,SGK,RUP,RB,ALP,ALB
  524 FORMAT(/  7H DRUP =F8.4,   5X 6HDALP = F9.4, /  6H SIP =F 9.4, 5X
     1   5HSGK =F10.4, 5X 5HRUP =F10.4, 5X 4HRB =F11.4,   5X 5HALP =F10.4,
     2  5X 5HALB =F10.4/  )
  525 CALL BAKER (     SGK,XB,YB,RB,ALB,A,B,R1B,AJ1B,R2B,AJ2B,.000001,
     1   A2,IT,C22,C23,NEXPR)
      DRUP=(RB-RUP)/(SGK-SIP)
      DALP=(ALB-ALP)/(SGK-SIP)
      SIP=SGK
      RUP=RB
      ALP=ALB
      IF(NEXPR) 527,527,526
  526 WRITE OUTPUT TAPE 2,524,DRUP,DALP,SIP,SGK,RUP,RB,ALP,ALB
  527 CONTINUE
      SNALB=YB/RB
      CNALB=XB/RB
      ALBD   =(180./3.141593)*   ALB
      XA=-XB
      YA=-YB
```

```
      ALA=ALB+3.141593
      RA=RB
      XI(20)=XA
      XI(40)=XB
      YI(20)=YA
      YI(40)=YB
      RI(20)=RA
      RI(40)=RB
      ALI(20)=ALA
      ALI(40)=ALB+6.283186
      VI(20)=0.
      VI(40)=0.
      R3B=-2.*(R1B*R2B-AJ1B*AJ2B)
      AJ3B=-2.*(AJ1B*R2B+R1B*AJ2B)
      DVXB=A*R3B-B*AJ3B
      DVYB=B*R3B+A*AJ3B
      DVZB=SQRTF(DVXB*DVXB+DVYB*DVYB)
      AHI(40)=ASINF(DVYB/DVZB)-1.5707965
      AHI(20)=AHI(40)+3.141593
      A22=A*A+B*B
      A23=R1*R1+AJ1*AJ1
      A24=R2*R2+AJ2*AJ2
      W2ZB=2.*SQRTF (A22*A23*A24)
      IF (NOPR)120,120,121
  120 WRITE OUTPUT TAPE 2, 122, BEJ,SNBE,CNBE,SGK,PHEB,A,B,XB,YB,RB,ALBC
     1, A2, IT
 1220FORMAT (1H1/// 46X 28HRESULTS IN NEAR CIRCLE PLANE //
     1    10X 6HBETA =F6.2, 5H DEG. 8X 10HSIN BETA = F7.4, 8X
     2    10HCOS BETA = F7.4, 8X 7HSIGMA = F7.3, /
     3    10X 8HPHI(B) = F8.4, 9X 3HA = F14.4, 8X 3HB = F14.4, //
     4    12X 1HI 9X 1HX 11X 1HY 11X 1HR 5X 12HLAMBDA, DEG.  6X 1HV
     5    6X 11HALPHA, DEG. 3X5HERROR 5X 10HITS  SHIFT //
     6    12X 1HO 3F12.4, F12.2, 6X 6H0.0000 8X4H*    E12.2, I6,
     7    6H        *)
  121 CONTINUE
C   PART IB POINTS ON NEAR CIRCLE
      DO 12 I=1,19
      IF(I-1) 13,13,14
   13 PHN=.9*PHEB
      AL=ALB+.45
      R=RB
      GO TO 15
   14 AI=I
      PHN=PHEB*(1.-AI/10.)
      AL=AL+(3.141593+ALB-AL)/(21.-AI)
   15 X=R*COSF(AL)
      Y=R*SINF(AL)
      CALL SSR(X,Y,VX,VY,V,C22,C23,A,B,PHN,PHEB,ITS,SNALB,CNALB,1.,
     1 ITSIDE,ERS,NEXPR)
      XI(I)=X
      YI(I)=Y
      R=SQRTF(X*X+Y*Y)
      RI(I)=R
      VI(I)=V
      AHI(I)=ATANF(VY/VX)
      IF(VX)49,50,50
   49 AHI(I)=AHI(I)+3.141593
   50 CONTINUE
      AHD     =(180./3.141593)*   AHI(I)
      AL=ATANF(Y/X)
      IF(X)36,37,37
   36 AL=AL+3.141593
   37 CONTINUE
      ALD     =(180./3.141593)*   AL
      ALI(I)=AL
      XI(I+20)=-(XI(I))
      YI(I+20)=-(YI(I))
      VI(I+20)=-(VI(I))
      ALI(I+20)=ALI(I)+3.141593
      AHI(I+20) = AHI(I)
```

```
      RI  (I+20) = RI(I)
      IF (NOPR) 124,124,12
  124 WRITE OUTPUT TAPE 2, 125,I,X,Y,R,ALD,V,AHD,ERS,ITS,ITSIDE
  125 FORMAT (II3,3F12.4, F12.2,F12.4,F12.2,E12.2,2I6)
   12 CONTINUE
   PART IIA  CONSTANTS FOR CIRCLE
      IF(NEXPR) 530,530,528
  528 WRITE OUTPUT TAPE 2, 529
  529 FORMAT (////)
  530 IT3=0
      POWER = (PHEB-2.*BE*SNBE)/CNBE
      DET=(2.*CNBE)/(EXPF(POWER)-1.)
   16 ARG 1 = 1.+(2.*CNBE)/DET
      ARG2 = SNBE/(CNBE+DET)
      PHE= CNBE*LOGF(ARG1)+SNBE*2.*ATANF(ARG2)
      ER3=PHE-PHEB
      RER3=ABSF(ER3)/PHEB
      IT3=IT3+1
      T=CNBE+DET
      Q1=CNBE+T
      Q2=1.+Q1*DET
      PHP=(-2./DET)*(T/Q1)*(T/Q2)
      DETNU = DET-ER3 /PHP
      IF(NEXPR) 516,516,505
  505 WRITE OUTPUT TAPE 2,506,IT3,DET,PHE,RER3,DETNU
  506 FORMAT(6H IT3 =I4,5X5HDET =E10.4,5X5HPHE =F10.6,5X6HRER3 =E10.4,
     1  5X7HDETNU =E10.4)
  516 IF(.000001-RER3) 17,19,19
   17 IF(IT3-25) 18,19,19
   18 IF(DETNU) 60,61,61
   60 DET=DET/2.
      GO TO 16
   61 DET=DETNU
      GO TO 16
   19 CH2G=1.+2.*Q1*DET
      SH2G=SQRTF (CH2G*CH2G-1.)
      SHG = SQRTF ((CH2G-1.)/2.)
      CHG = SQRTF ((CH2G+1.)/2.)
      C2=CH2G
      C3=SH2G
      C4=SHG
      C5=CHG
      TEB=ATANF((C4/C5)*(C22/C23))
      TEBD    =(180./3.141593)*           TEB
      CNTEB=COSF(TEB)
      TEA=TEB+3.141593
      TEI(20)=TEA
      TEI(40)=TEB+6.283186
     .VTB=0.
      VTA=0.
      DVB=-(C3)/(C2-COSF(2.*TEB))
      DVA=DVB
      VTI(20)=0.
      VTI(40)=0.
      DVI(20)=DVA
      DVI(40)=DVB
      A22=C23*C5*CCSF(TEB)
      A23=C22*C4*SINF(TEB)
      A24=C2-COSF(2.*TEB)
      W2TB=4.*(A22+A23)/A24
      IF (NOPR) 126,126,128
 1260WRITE OUTPUT TAPE 2, 127,SHG,CHG,DET,PHP,TEBD,DVB,RER3,IT3
 1270FORMAT(//41X37HCORRESPONDING RESULTS IN CIRCLE PLANE//
     1   10X 12HSINH GAMMA = F8.4, 5X 12HCOSH GAMMA = F8.4, 5X 7HDEL T =
     2   E10.4,   8X  11HPHI PRIME = E10.4, //
     3   15X 1HI 9X 11HTHETA, DEG. 11X 7HV THETA 10X 13HDELTA V THETA 10X
     4   5HERROR 11X 3HITS // 15X 1H0 F17.2,   15X   6H0.0000 F20.4,
     5   E19.2, I13)
  128 CONTINUE
C   PART IIB  POINTS ON CIRCLE
```

75

```
      DO 20 I=1,19
      AI=I
      PHN=PHEB*(1.-AI/10.)
      IF(I-1)21,21,22
   21 TEOLD = TEB
      TE = TEB + SCRTF (.2*PHEB/W2TB)
      GO TO 23
   22 TEOLD = TE
      TENU 1 = TE-.1*PHEB/VTE
      IF (TEA-TENU 1) 53,53,54
   53 TE = (TE+TEA)/2.
      GO TO 23
   54 TE = TENU 1
   23 IT4=0
   25 C6=SINF(TE)
      C7=COSF(TE)
      C8=COSF(2.*TE)
      A2=LOGF((C5+C7)/(C5-C7))
      A3=2.*ATANF(C6/C4)
      PH=C23*A2+C22*A3
      A2=-(C23*C5*C6)+C22*C4*C7
      VTE=4.*A2/(C2-C8)
      DPH=PH-PHN
      IT4=IT4+1
      A2=ABSF(DPH)/PHEB
      IF(NEXPR) 511,511,512
  512 WRITE OUTPUT TAPE 2, 513, I, IT4, TE,DPH,VTE,A2
  513 FORMAT (   6H    I =I4, 5X5HIT4 =I4, 6X4HTE =E10.4, 6X5HDPH =E10.4,
     1 5X5HVTE =E10.4, 5X4HA2 =E10.4)
  511 IF(IT4-25) 24,111,111
   24 IF ( .000001 - A2) 26, 111, 111
   26 TENU = TE-DPH/VTE
      IF (TENU - TEOLD ) 51,51,55
   51 TE = (TE+TEOLD)/2.
      GO TO 25
   55 IF (TEA-TENU) 56,56,57
   56 TE = (TE+TEA)/2.
      GO TO 25
   57 TE = TENU
      GO TO 25
  111 TED      =(180./3.141593)*   TE
      TEI(I) = TE
      VTI(I)=VTE
      DVI(I)=-C3/(C2-C8)
      TEI(I+20)=TEI(I)+3.141593
      VTI(I+20)=-(VTI(I))
      DVI(I+20) = DVI(I)
      IF (NOPR) 129,129,20
  129 WRITE OUTPUT TAPE 2, 130,I,TED,VTE,DVI(I),A2,IT4
  130 FORMAT (I16, F17.2, F21.4, F20.4, E19.2, I13)
   20 CONTINUE
C  PARTIIIA  CONSTANTS FOR AIRFOIL
      BZL=BZ1
      DO29L=1,NBZ
      BAM=ABSF(BZL)
      IF(BAM-.001)85,85,86
   85 TAU=0.
      XT=XB
      YT=YB
      XI(42)=XT
      YI(42)=YT
      VT=0.
      AHT=AHI(40)
      AHL=AHI(20)
      AHI(41)=AHL
      AHI(42)=AHT
      TET=TEB+6.283186
      PHT=PHEB
      XL=XA
      YL=YA
```

```
      XI(41)=XL
      YI(41)=YL
      VL=0.
      TEL=TEA
      PHL=-PHEB
      GO TO 87
86    CONTINUE
      C2=CH2G
      C3=SH2G
      C4=SHG
      C5=CHG
      C22=SNBE
      C23=CNBE
      TAU=ASINF((BZL/4.)*(SH2G/CHG)*(CNTEB/CNBE))
      TET=TEB-TAU+6.283186
      TEL=TEA+TAU
      A2=SINF(TET)
      A3=COSF(TET)
      A4=(C5+A3)/(C5-A3)
      A5=A2/C4
      PHT=C23*LOGF(A4)+C22*2.*ATANF(A5)
      A2=SINF(TEL)
      A3=COSF(TEL)
      A4=(C5+A3)/(C5-A3)
      A5=A2/C4
      PHL=C23*LOGF(A4)+C22*2.*ATANF(A5)
      ENT=30.+10.*PHT/PHEB
      I=39
32    AI=I
      IF(ENT-AI) 3C,31,31
30    I=I-1
      GO TO 32
31    A2=(TET-TEI(I))/(TEI(I+1)-TEI(I))
      RT=RI(I)+A2*(RI(I+1)-RI(I))
      ALT=ALI(I)+A2*(ALI(I+1)-ALI(I))
      XT=RT*COSF(ALT)
      YT=RT*SINF(ALT)
      ENL=30.+10.*PHL/PHEB
      I=21
33    AI=I
      IF(AI-ENL)34,35,35
34    I=I+1
      GOTO33
35    A2=(TEL-TEI(I))/(TEI(I+1)-TEI(I))
      RL=RI(I)+A2*(RI(I+1)-RI(I))
      ALL=ALI(I)+A2*(ALI(I+1)-ALI(I))
      XL=RL*COSF(ALL)
      YL=RL*SINF(ALL)
      CALL SSR(XT,YT,VX,VY,VT,C22,C23,A,B,PHT,PHEB,ITS,SNALB,CNALB,-1.,
     1 ITSIDE,ERST,NEXPR)
      XI(42)=XT
      YI(  42)= YT
      AHT=ATANF(VY/VX)
      IF(VX)63,64,64
63    AHT=AHT+3.141593
64    AHI(42)=AHT
      CALLSSR(XL,YL,VX,VY,VL,C22,C23,A,B,PHL,PHEB,ITS,SNALB,CNALB,-1.,
     1 ITSIDE,ERSL,NEXPR)
      XI(41)=XL
      YI(41)=YL
      AHL=ATANF(VY/VX)
      IF(VX)65,66,66
65    AHL=AHL+3.141593
66    AHI(41)=AHL
87    CONTINUE
      TNBE=SNBE/CNBE
      TNBE2=TNBE-BZL/2.
      CV2=(1.+TNBE*TNBE)/(1.+TNBE2*TNBE2)
      CV=SQRTF(CV2)
      EPM=EP1
```

```
      DO 40 M=1,NEP
      AKN=AK1
      DO 41 N=1,NAK
      IF(EPM) 99,98,99
   98 IF(N-1) 99,99,41
   99 CONTINUE
      XP=XL-EPM*RB*SINF(AHL)
      YP=YL+EPM*RB*COSF(AHL)
      XQ=XT-AKN*EPM*RB*SINF(AHT)
      YQ=YT+AKN*EPM*RB*COSF(AHT)
      XZ=(XP+XQ)/2.
      YZ=(YP+YQ)/2.
      XQP=XQ-XZ
      YQP=YQ-YZ
      X=XQP
      Y=YQP
      C2=SINH(X)
      C3=COSH(X)
      C6=SINF(Y)
      C7=COSF(Y)
      R1=(C2/(C3-C7))/2.
      AJ1=(C6/(C3-C7))/(-2.)
      PX=C3*C7-1.
      PY=C2*C6
      PZ=PX*PX+PY*PY
      R2=PX/(PZ*(-2.))
      AJ2=PY/(PZ*2.)
      QZ=R2*R2+AJ2*AJ2
      PU=Y*QZ-R2*AJ1+AJ2*R1
      PV=X*QZ-AJ2*AJ1-R2*R1
      BEP=ATANF(PU/PV)
      C22=SINF(BEP)
      C23=COSF(BEP)
      QX=AJ2*C22-R2*C23
      QY=R2*C22+AJ2*C23
      AP=QX/QZ
      BP=QY/QZ
      AP22=AP*AP+BP*BP
      AP23=R1*R1+AJ1*AJ1
      AP24=R2*R2+AJ2*AJ2
      WP2ZB=2.*SQRTF(AP22*AP23*AP24)
C  PARTIIIB  POINTS ON AIRFOIL
      I=1
   42 X=XI(I)-XZ
      Y=YI(I)-YZ
      C2=SINH(X)
      C3=COSH(X)
      C6=SINF(Y)
      C7=COSF(Y)
      R1=C2/(2.*(C3-C7))
      AJ1=C6/(-2.*(C3-C7))
      PX=C3*C7-1.
      PY=C2*C6
      PZ=PX*PX+PY*PY
      R2=PX/(PZ*(-2.))
      AJ2=PY/(2.*PZ)
      XII(I)=X*C23+Y*C22+AP*R1-BP*AJ1
      ETI(I)=-X*C22+Y*C23+AP*AJ1+BP*R1
      A2=C23+AP*R2-BP*AJ2
      A3=C22-AP*AJ2-BP*R2
      A4=SQRTF(A2*A2+A3*A3)
      IF(A4-.0001) 171,171,172
  171 RP3=-2.*(R1*R2-AJ1*AJ2)
      AJP3=-2.*(AJ1*R2+R1*AJ2)
      DUXP=AP*RP3-BP*AJP3
      DUYP=BP*RP3+AP*AJP3
      DUP=SQRTF(DUXP*DUXP+DUYP*DUYP)
      EPI(I)=ASINF(DUYP/DUP)-1.5707965
      IF(ALI(I)-ALI(30)) 173,173,113
  173 EPI(I)=EPI(I)+3.141593
```

```
      GO TO 113
172   EPI(I)=ASINF (A3/A4)
      IF(A2) 600,113,113
600   EPI(I)=3.141593-EPI(I)
113   DELI(I)=(180./3.141593)*(AHI(I)-EPI(I))
      A6=ABSF(VTI(I))
      IF(A6-.0001) 88,88,89
 88   A5=SQRTF(W2ZB/W2TB)
      GO TO 38
 89   A5=VI(I)/VTI(I)
 38   IF(ABSF(A4)-.0001) 39,39,59
 39   IF(BAM-.0001) 43,43,44
 43   VVI(I)=SQRTF(W2ZB/WP2ZB)
      GO TO 62
 44   R3=-2.*(R1*R2-AJ1*AJ2)
      AJ3=-2.*(AJ1*R2+R1*AJ2)
      WP2Z=SQRTF(AP22*(R3*R3+AJ3*AJ3))
      SHX=SINH(XI(I))
      CHX=COSH(XI(I))
      SNY=SINF(YI(I))
      CNY=COSF(YI(I))
      R1=(SHX/2.)/(CHX-CNY)
      AJ1=(-SNY/2.)/(CHX-CNY)
      PX=CHX*CNY-1.
      PY=SHX*SNY
      PZ=PX*PX+PY*PY
      R2=PX/(-2.*PZ)
      AJ2=PY/(2.*PZ)
      R3=-2.*(R1*R2-AJ1*AJ2)
      AJ3=-2.*(AJ1*R2+R1*AJ2)
      W2Z=SQRTF((A*A+B*B)*(R3*R3+AJ3*AJ3))
      SNTE=SINF(TEI(I))
      CNTE=COSF(TEI(I))
      SN2TE=SINF(2.*TEI(I))
      CN2TE=COSF(2.*TEI(I))
      B22=CNBE*CHG*CNTE
      B23=SNBE*SHG*SNTE
      B24=CH2G-CN2TE
      W2T=-4.*(B22+B23)/B24
      DW2T=(2.*SH2G*SN2TE)/(B24*B24)
      A25=W2Z-A5*A5*W2T
      A26=(DVI(I)*A25)/A6-A5*A5*DW2T
      VVI(I)=(W2Z+BZL*A26)/WP2Z
      GO TO 62
 59   VVI(I)=(VI(I)+BZL*DVI(I)*A5)/A4
 62   IF(I-42) 46,47,47
 46   I=I+1
      GOTO42
 47   CONTINUE
      DELX=XII(42)-XII(41)
      DELY=ETI(42)-ETI(41)
      CHORD=SQRTF(DELX*DELX+DELY*DELY)
      SOLID=CHORD/6.283186
      SNA=DELY/CHORD
      CNA=DELX/CHORD
      AROT=(180./3.141593)*ASINF (SNA)
      STAG=(180./3.141593)*(BEP+ASINF(SNA))
      AHTD    =(18C./3.141593)* AHT
      TE-TD   =(18C./3.141593)* TET
      AHLD    =(18C./3.141593)* AHL
      TELD    =(18C./3.141593)*  TEL
      TAUD    =(180./3.141593)*  TAU
      BEPD    =(180./3.141593)* BEP
710   IAA= 20
      DO 717 IDD=1, 1C
      IAA =IAA-1
716   I= 35
      TDD=TANF (DELI(IAA)*3.141593/180.)
715   AA= XNI(I)-XNI(IAA) - (YNI(IAA)-YNI(I))*TDD
      IF (AA) 714,714,713
```

79

```
713 I=I-1
    GO TO 715
714 BBE=ATANF ((YNI(I+1) -YNI(I))/(XNI(I+1)-XNI(I)))
    DDEL = .5*(BBE+DELI(IAA)*3.141593/180.)
    CC = ABSF((YNI(IAA)-YNI(I+1))/COSF(DDEL))
717 DDI(IDD) = CC+ (XNI(I+1)- XNI (IAA) -(YNI(IAA) - YNI(I+1))*
   1    TANF(DDEL))*SINF (BBE )
    WAXIE = DDI(1)
    DO 718   IDD = 2,10
718 WAXIE = MAXIF (WAXIE, DDI(IDD))
    WRITE OUTPUT TAPE 2,302, BEJ,SGK,BZL,EPM,AKN,STAG,SOLID,WAXIE
302 FORMAT (1H1//52X15HCASCADE RESULTS//
   1    18H DESIGN PARAMETERS/
   2    9H    BETA =F6.2, 5H DEG. 6X7HSIGMA = F6.3,10X8HB ZERO =
   3    F6.2, 9X 9HEPSILON = F5.3,9X7HKAPPA = F6.3,//
   4    17H OTHER PARAMETERS/
   5    11H    STAGGER=F6.2,5H DEG. 4X 10HSOLIDITY =F6.3 ,7X17HMAX. THI
   6CKNESS = F5.3)
    IF (NDPR) 140,140,141
140 WRITE OUTPUT TAPE 2,304, XB,YB,PHEB,XT,YT,AHTO,TETD,PHT,XL,YL,AHLO,
   1    TELD,PHL,XP,YP,XQ,YQ,TAUD,XZ,YZ,AP,BP,BEPD
3040FORMAT (3X4HXB =F8.4,11X4HYB =F8.4, 11X8HPHI(B) =F8.4,/3X
   1    4HXT = F8.4,11X4HYT =F8.4, 11X10HALPHA(T) = F6.2, 5H DEG.
   2    2X10HTHETA(T) = F6.2, 5H DEG. 2X8HPHI(T) = F8.4,/3X
   3    4HXL = F8.4, 11X4HYL = F8.4, 11X10HALPHA(L) = F6.2, 5H DEG.
   4    2X10HTHETA(L) = F6.2, 5H DEG. 2X 8HPHI(L) = F8.4,/3X
   5    4HXP =F8.4,11X4HYP =F8.4,11X4HXQ =F8.4,11X4HYQ =F8.4,11X
   6    5HTAU =F13.2, 5H DEG.,/3X
   7    4HXZ = F8.4, 11X4HYZ = F8.4, 11X4HAP = F8.4, 11X4HBP = F8.4,11X
   8    12HBETA PRIME = F6.2, 5H DEG.)
141 WRITE OUTPUT TAPE 2,303
3030FORMAT (//42X 13HAIRFOIL SHAPE 32X21HVELOCITY DISTRIBUTION/
   1    88X 19HAT DESIGN CONDITION/
   2    10X1HI17X1HX19X1HY14X11HSLOPE, DEG.11X6H(V/V2) 12X9H(V/V2)**2//)
    I=1
    DO 90 I=1,42
    PRX=(XII(I)-XII(41))/CHORD
    PRY=(ETI(I)-ETI(41)) /CHORD
    XNI(I)=PRX*CNA+PRY*SNA
    YNI(I)=PRY*CNA-PRX*SNA
    DELI(I)=DELI(I)-AROT
    VVI(I)=CV*VVI(I)
    V2I(I) = VVI(I)*VVI(I)
 90 CONTINUE
    WRITEOUTPUTTAPE2,305,(I,XNI(I),YNI(I),DELI(I),VVI(I),V2I(I),
   1I=1,42)
305 FORMAT (I11, 2F20.4, F20.2, 2F20.4)
C   PARTIV   PARAMETER CHANGES
 48 AKN=AKN+AKI
 41 CONTINUE
    EPM=EPM+EBI
 40 CONTINUE
    BZL=BZL+BZI
 29 CONTINUE
    SGK=SGK+SGI
  3 CONTINUE
    BEJ=BEJ+BEI
  2 CONTINUE
    ID=ID+1
    IF(IB-ID) 203,203,202
203 END
C   PART V   ITERATION SUBROUTINE FOR POINTS ON NEAR CIRCLE
    SUBROUTINE SSR (X,Y,VX,VY,V,C22,C23,A,B,PHN,PHEB,ITS,SNALB,CNALB,
   1SIDE,ITSIDE,A2, NEXPR)
    ITS=0
    ITSIDE=0
    IF(NEXPR) 8,8,517
517 WRITE OUTPUT TAPE 2,510
510 FORMAT(//5H   ITS 4X1HX 9X1HY 9X2HR1 7X3HAJ1 8X2HR2 7X3HAJ28X1HA
   1   9X1HB 8X2HVX  8X2HVY  8X2HA2  5X4HSIDE/)
```

80

```
   8 C2=SINH(X)
     C3=COSH(X)
     C6=SINF(Y)
     C7=COSF(Y)
     A2=C3-C7
     R1=C2/(A2*2.)
     AJ1=C6/(A2*(-2.))
     PX=C3*C7-1.
     PY=C2*C6
     PZ=PX*PX+PY*PY
     R2=PX/(-2.*PZ)
     AJ2=PY/(2.*PZ)
     PH=X*C23+Y*C22+A*R1-B*AJ1
     PS=-X*C22+Y*C23+A*AJ1+B*R1
     DPH=PH-PHN
     VX=C23+A*R2-B*AJ2
     VY=C22-A*AJ2-B*R2
     V=-SIDE*SQRTF(VX*VX+VY*VY)
     A2=(ABSF(DPH)+ABSF(PS))/PHEB
     ITS=ITS+1
     IF(NEXPR) 507,507,508
 508 WRITE OUTPUT TAPE 2,509,ITS,X,Y,R1,AJ1,R2,AJ2,A,B,VX,VY,A2,ITSIDE
 509 FORMAT (I5, 10F10.4, E10.4, I5)
 507 IF(ITS-25) 9,100,100
   9 IF (.000001-A2) 10,100,100
  10 DX=(VX*DPH-VY*PS)/(V*V)
     DY=(VY*DPH+VX*PS)/(V*V)
     X=X-DX
     Y=Y-DY
     GO TO 8
 100 YY=Y*CNALB-X*SNALB
     IF (YY*SIDE)101,11,11
 101 ITSIDE=ITSIDE+1
     IF(ITSIDE-3) 102,11,11
 102 YY=-YY
     XX=X*CNALB+Y*SNALB
     X=XX*CNALB-YY*SNALB
     Y=YY*CNALB+XX*SNALB
     GO TO 8
  11 RETURN
     END
C  PART VI ITERATION SUBROUTINE FOR INITIAL STAGNATION POINTS ON NEAR CIRCLI
     SUBROUTINE BAKER (    SGK,XB,YB,RB,ALB,A,B,R1,AJ1,R2,AJ2,ERM,A2,
    1    IT,C22,C23,NEXPR)
     IF(NEXPR)515,515,500
 500 WRITE OUTPUT TAPE 2,501
 501 FORMAT(//5H    IT 4X2HXB 8X2HYB 8X2HR1 7X3HAJ1 8X2HR2 7X3HAJ2 8X1HA
    1  9X1HB 9X2HPS 8X2HDP 8X2HA2/)
 515 CONTINUE
     IT=0
     PHEB=SGK*3.141593
     SNALB= SINF(ALB)
     CNALB= COSF(ALB)
     XB=RB*CNALB
     YB=RB*SNALB
   4 C2=SINH(XB)
     C3=COSH(XB)
     C6=SINF(YB)
     C7=COSF(YB)
     A2=C3-C7
     R1=C2 /(A2*2.)
     AJ1=C6/(A2*(-2.))
     PX=C3*C7-1.
     PY=C2*C6
     PZ=PX*PX+PY*PY
     R2=PX/(PZ*(-2.))
     AJ2=PY/(PZ*2.)
     QX=AJ2*C22-R2*C23
     QY=AJ2*C23+R2*C22
     QZ=R2*R2+AJ2*AJ2
```

81

```
      A=QX/QZ
      B=QY/QZ
      PH=XB*C23+YB*C22+A*R1-B*AJ1
      PS=-XB*C22+YB*C23+A*AJ1+B*R1
      DP=PH-PHEB
      A2=(ABSF(DP)+ABSF(PS))/PHEB
      IT=IT+1
      IF(NEXPR) 514,514,503
  503 WRITE OUTPUT TAPE 2,504,IT,XB,YB,R1,AJ1,R2,AJ2,A,B,PS,DP,A2
  504 FORMAT (I5,1CF10.4,1E10.4)
  514 CONTINUE
      IF(IT-25) 5,7,7
    5 IF(ERM-A2) 6,7,7
    6    A2*C3-C7
      R1X=(1.-C3*C7)/(A2*A2*2.)
      R1Y=(C2*C6)/(A2*A2*(-2.))
      AJ1X=-R1Y
      AJ1Y=R1X
      PXX=C2*C7
      PXY=-C3*C6
      PYX=-PXY
      PYY=PXX
      PZX=2.*(PX*PXX+PY*PYX)
      PZY=2.*(PX*PXY+PY*PYY)
      R2X=(PZ*PXX-PX*PZX)/((PZ*PZ)*(-2.))
      R2Y=(PZ*PXY-PX*PZY)/(PZ*PZ*(-2.))
      AJ2X=-R2Y
      AJ2Y=R2X
      QXX=-R2X*C23+AJ2X*C22
      QXY=-R2Y*C23+AJ2Y*C22
      QYX=QXY
      QYY=-QXX
      QZX=2.*(R2*R2X+AJ2*AJ2X)
      QZY=2.*(R2*R2Y+AJ2*AJ2Y)
      AX=(QZ*QXX-QX*QZX)/(QZ*QZ)
      AY=(QZ*QXY-QX*QZY)/(CZ*QZ)
      BX=(QZ*QYX-QY*QZX)/(QZ*QZ)
      BY=(QZ*QYY-QY*QZY)/(QZ*QZ)
      PHX=C23+A*R1X+AX*R1-B*AJ1X-BX*AJ1
      PHY=C22+A*R1Y+AY*R1-B*AJ1Y-BY*AJ1
      PSX=-C22+A*AJ1X+AX*AJ1+B*R1X+BX*R1
      PSY=C23+A*AJ1Y+AY*AJ1+B*R1Y+BY*R1
      A2=PHX*PSY-PSX*PHY
      DX=(PSY*DP -PHY*PS)/A2
      DY=(PHX*PS-PSX*DP )/A2
      XB=XB-DX
      YB=YB-DY
      GO TO 4
    7 RB=SQRTF(XB*XB+YB*YB)
      ALB=ATANF(YB/XB)
      IF(XB)28,45,45
   28 ALB=ALB+3.141593
   45 CONTINUE
      RETURN
      END
      END
1 5 6 1 5 45. 2.5    .5   .001  .01  0      .4    .15   0    .245   1 0
```

..END
```

```
C   PART IA CONSTANTS FOR NEAR CIRCLE
        BEJ=BE1
        DO2 J=1,NBE
        BE= (3.141593/180.) * BEJ
        SNBE=SINF(BE)
        CNBE=COSF(BE)
        SGK=SG1
        DO3 K=1,NSG
    740 WRITE OUTPUT TAPE 2, 741, BEJ, SGK
    741 FORMAT (1H1/26HCASCADE RESULTS FOR BETA =F6.2,5H DEG.4X7HSIGMA =
       1F6.3,//75H   B ZERO      KAPPA      EPSILON      SOLIDITY      THICKNE
       2SS    BL PARAMETER/)
```

```
        DO 718   IDD = 2,10
    718 WAXIE = MAX1F (WAXIE, DDI(IDD))
    751 PRAM= V2I(1)
        DO 760 I= 1, 19
    760 PRAM = MAX1F (PRAM, V2I(I))
        WRITE OUTPUT TAPE 2, 755, BZL, AKN, EPM, SOLID, WAXIE, PRAM
    755 FORMAT (3X,F6.2,2F10.3,2F14.3,F16.4)
C   PARTIV PARAMETER CHANGES
```

```
   87 CONTINUE
      TNBE=SNBE/CNBE
      TNBE2=TNBE-BZL/2.
      CV2=(1.+TNBE*TNBE)/(1.+TNBE2*TNBE2)
      CV=SQRTF(CV2)
    . AKN=AK1
      DO 41 N=1,NAK
      WAXIT = 0
      THIK = .04
      EPM=EP1
      IF(EPM) 99,98,99
   98 IF(N-1) 99,99,41
   99 CONTINUE
```

```
    1    TANF(DDEL))*SINF (BBE )
      WAXIE = DDI(1)
      DO 718   IDD = 2, 10
  718 WAXIE = MAXIF (WAXIE, DDI(IDD))
  756 IF (WAXSG) 757, 757, 751
  757 IF (THIK - WAXIE) 761, 751, 763
  761 IF (WAXIT) 764, 764, 765
  764 EPM = EPM - .01
      GO TO 99
  765 EPM = EPM - .01*((WAXIE - THIK)/(WAXIE - WAXIT))
      WAXSG = 100.0
      GO TO 99
  763 EPM = EPM + .01
      WAXIT = WAXIE
      GO TO 99
  751 PRAM= V2I(1)
      DO 760 I= 1, 19
  760 PRAM = MAXIF (PRAM, V2I(I))
      WRITE OUTPUT TAPE 2, 755, BZL, AKN, EPM, SOLID, WAXIE, PRAM
  755 FORMAT (3X,F6.2,2F10.3,2F14.3,F16.4)
      EPM=EPM+EBI
      THIK = THIK + .04
      WAXIT = 0
      WAXSG = 0
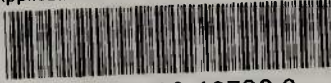      IF (THIK - .25) 99, 99, 48
C  PARTIV  PARAMETER CHANGES
   48 AKN=AKN+AKI
   41 CONTINUE
      BZL=BZL+BZI
   29 CONTINUE
      SGK=SGK+SGI
    3 CONTINUE
      BEJ=BEJ+BEI
    2 CONTINUE
      ID=ID+1
      IF(IB-ID) 203,203,202
  203 END
```